

POWER DIAGRAMS AND INTERACTION PROCESSES FOR UNIONS OF DISCS

JESPER MØLLER,* *Aalborg University*

KATEŘINA HELISOVÁ,** *Charles University in Prague*

Abstract

We study a flexible class of finite-disc process models with interaction between the discs. We let \mathcal{U} denote the random set given by the union of discs, and use for the disc process an exponential family density with the canonical sufficient statistic depending only on geometric properties of \mathcal{U} such as the area, perimeter, Euler–Poincaré characteristic, and the number of holes. This includes the quermass–interaction process and the continuum random-cluster model as special cases. Viewing our model as a connected component Markov point process, and thereby establishing local and spatial Markov properties, becomes useful for handling the problem of edge effects when only \mathcal{U} is observed within a bounded observation window. The power tessellation and its dual graph become major tools when establishing inclusion–exclusion formulae, formulae for computing geometric characteristics of \mathcal{U} , and stability properties of the underlying disc process density. Algorithms for constructing the power tessellation of \mathcal{U} and for simulating the disc process are discussed, and the software is made public available.

Keywords: Area–interaction process; Boolean model; disc process; exponential family; germ–grain model; local computations; local stability; Markov properties; inclusion–exclusion formulae; interaction; point process; power tessellation; simulation; quermass–interaction process; random closed set; Ruelle stability

2000 Mathematics Subject Classification: Primary 60D05; 60G55; 60K35; 62M30
Secondary 68U20

1. Introduction

This paper concerns probabilistic results of statistical relevance for planar random set models given by a finite union of discs $\mathcal{U} = \mathcal{U}_X$, where X denotes the corresponding finite process of discs. We distinguish between the case where we can observe the discs in X and the random set case where only (or at most) \mathcal{U} is observed. The latter case occurs frequently in applications and will be of main interest to us.

Our random closed set \mathcal{U} is a particular example of a germ–grain model [17], with the grains being discs. It is well known that any random closed set whose realizations are locally finite unions of compact convex sets is a germ–grain model with convex and compact grains [43], [44]. However, in order to make statistical inference, we need to restrict attention to a much smaller class of models such as a random-disc process model, and indeed random-disc Boolean models play the main role in practice (see [41] and the references therein). The Boolean model is in an abstract setting given by a Poisson process of compact sets (the grains) with no interaction

Received 21 August 2007; revision received 1 February 2008.

* Postal address: Department of Mathematical Sciences, Aalborg University, Fredrik Bajers Vej 7G, DK-9220 Aalborg, Denmark. Email address: jm@math.aau.dk

** Postal address: Department of Probability and Mathematical Statistics, Charles University in Prague, Sokolovská 83, 18675 Praha 8, Czech Republic. Email address: helisova@karlin.mff.cuni.cz

between the grains. Many authors (see, for example, [2], [8], [9], [16], [22], and [41]) have mentioned the need of developing flexible germ–grain models with interaction between the grains.

We study a particular class of models for interaction among the discs, specified by a point process density for X with respect to a reference Poisson process of discs. The density is assumed to be of exponential family form with the canonical sufficient statistic $T(X) = T(\mathcal{U})$ depending only on X through \mathcal{U} , where $T(\mathcal{U})$ is specified in terms of geometric characteristics for the connected components of \mathcal{U} , for example, the area $A(\mathcal{U})$, the perimeter $L(\mathcal{U})$, the number of holes $N_h(\mathcal{U})$, and the number of connected components $N_{cc}(\mathcal{U})$. Further geometric characteristics are specified in Section 4.1 in terms of the power tessellation (see, for example, [1]), which provides a subdivision of \mathcal{U} (see Figure 1 in Section 3). An important special case of our models is the quermass-interaction process, first introduced in [22], where

$$T(\mathcal{U}) = (A(\mathcal{U}), L(\mathcal{U}), \chi(\mathcal{U})) \quad \text{and} \quad \chi(\mathcal{U}) = N_{cc}(\mathcal{U}) - N_h(\mathcal{U})$$

is the Euler–Poincaré characteristic (quermass integrals in \mathbb{R}^2 are linear combinations of A , L , and χ). Another special case is the continuum random-cluster model [15], [23], [28], where $T(\mathcal{U}) = N_{cc}(\mathcal{U})$.

We show that the power tessellation and its dual graph are extremely useful when establishing

- (i) inclusion–exclusion formulae for $T(\mathcal{U})$;
- (ii) formulae for computing geometric characteristics of \mathcal{U} ;
- (iii) Ruelle stability and local stability of the density of X , and thereby convergence properties of Markov chain Monte Carlo (MCMC) algorithms for simulating X .

Note that the use of power diagrams is confined to discs (or balls), while, for example, quermass-interaction processes for other types of grains have been studied in the literature. Among other things, we demonstrate that a main geometric result in [22] related to the issue of Ruelle stability is easily derived by means of the power tessellation and its dual graph. Furthermore, as explained in Section 4.5, it becomes useful to view our models as connected component Markov point processes [2], [4], [7], [30] in a similar way as the Markov connected component fields studied in [33]. In particular, we establish

- (iv) local and spatial Markov properties of X , which become useful for handling the problem of edge effects when only \mathcal{U} is observed within a bounded observation window.

The paper is organized as follows. In Section 2 we specify our notation and assumptions, and discuss a general position property of the discs in X . In Section 3 we define and study the power tessellation of a union of discs in general position. In the main section, Section 4, we study exponential family properties and the abovementioned issues (i)–(iv). Also, various examples of simulated realizations of our models are shown in Section 4. In Section 5 we discuss extensions of our work and some open problems. Finally, most algorithmic details are deferred to Appendix A.

A substantial part of this work has been the development of codes in C and R for constructing power tessellations and making simulations of our models. The codes are available at www.math.aau.dk/~jm/Codes.union.of.discs.

2. Preliminaries

2.1. Setup

Throughout this paper, we use the following notation and make the following assumptions. By a disc we mean more precisely a two-dimensional closed disc

$$b = \{y \in \mathbb{R}^2 : \|y - z\| \leq r\}$$

with center $z \in \mathbb{R}^2$ and positive radius $r > 0$, where $\|\cdot\|$ denotes the usual Euclidean distance. We identify b with the point $x = (z, r)$ in $\mathbb{R}^2 \times (0, \infty)$ and write $b = b(x) = b(z, r)$. Similarly, we identify point processes of discs $b_i = b(z_i, r_i)$ with point processes on $\mathbb{R}^2 \times (0, \infty)$.

The reference point process will be a Poisson process Ψ of discs; thus, the random set given by the union of discs in Ψ is a Boolean model (see, for example, [27]). Specifically, Ψ is assumed to be a Poisson point process on $\mathbb{R}^2 \times (0, \infty)$ with an intensity measure of the form $\rho(z) dz Q(dr)$, where dz is the Lebesgue measure on \mathbb{R}^2 and Q is an arbitrary probability measure on $(0, \infty)$. In other words, the point process Φ of centers of discs given by Ψ is a Poisson process with intensity function ρ on \mathbb{R}^2 , the radii of these discs are mutually independent and identically distributed with distribution Q , and Φ is independent of the radii. (An example of a simulation from such a process is shown in Figure 3(a)). The concrete specification of ρ and Q is not important for most results in this paper, but the specification is of course crucial for statistical inference (see [32]). Local integrability of ρ is assumed to ensure that, with probability 1, $\Phi \cap S$ is finite for any bounded region $S \subset \mathbb{R}^2$. Since we can view the radii as marks associated to the points given by the centers of the discs, we refer to Q as the *mark distribution*. In the special case where Q is degenerate at $R > 0$, we can consider R as a parameter and identify Ψ with Φ .

In the sequel S denotes a given bounded planar region such that $\int_S \rho(z) dz > 0$. The object of primary interest is the random closed set

$$\mathcal{U}_X = \bigcup_{x \in X} b(x),$$

where X is a finite point process defined on $S \times (0, \infty)$. If $X = \emptyset$ is the empty configuration, we let $\mathcal{U}_X = \emptyset$ be the empty set. Note that the centers of the discs are contained in S , but the discs may extend outside S . We assume that X is absolutely continuous with respect to the reference Poisson process Ψ , and denote the density by $f(x)$ for finite configurations $x = \{x_1, \dots, x_n\}$ with $x_i = (z_i, r_i) \in S \times (0, \infty)$ and $0 \leq n < \infty$ (if $n = 0$ then x is the empty configuration).

We focus on the case where the density is of the exponential family form, i.e.

$$f_\theta(x) = \frac{\exp(\theta \cdot T(\mathcal{U}_x))}{c_\theta}, \tag{1}$$

where θ is a real parameter vector, \cdot denotes the usual inner product, $T(\mathcal{U})$ is a statistic of the same dimension as θ , and c_θ is a normalizing constant depending on θ (and of course also on (T, ρ, Q)). Note that $f_\theta(x) > 0$ for all x . Further details on the choice of T and the parameter space for θ are given in Section 4. Note that (1) is also the density of the random set \mathcal{U}_X with

respect to the reference Boolean model and that

$$\begin{aligned}
 c_\theta &= \exp\left(-\int_S \rho(z) dz\right) \\
 &\times \left(\exp(\theta \cdot T(\emptyset)) + \sum_{n=1}^\infty \frac{1}{n!} \int_S \int_0^\infty \cdots \int_S \int_0^\infty \exp(\theta \cdot T(\mathcal{U}_{\{(z_1,r_1),\dots,(z_n,r_n)\}})) \right. \\
 &\quad \left. \times \prod_1^n \rho(z_i) dz_1 Q(dr_1) \cdots dz_n Q(dr_n)\right) \tag{2}
 \end{aligned}$$

is in general not expressible in closed form (unless $\theta = \mathbf{0}$).

As noted in Section 1, a quermass-interaction process is obtained by taking $T(\mathcal{U}) = (A(\mathcal{U}), L(\mathcal{U}), \chi(\mathcal{U}))$, where $A(\mathcal{U})$ is the area, $L(\mathcal{U})$ is the perimeter, and $\chi(\mathcal{U})$ is the Euler–Poincaré characteristic of \mathcal{U} . We consider here the so-called additive extension of the Euler–Poincaré characteristic, which is also of primary interest in [22], i.e.

$$\chi(\mathcal{U}) = N_{cc}(\mathcal{U}) - N_h(\mathcal{U}), \tag{3}$$

where $N_{cc}(\mathcal{U})$ is the number of connected components of \mathcal{U} and $N_h(\mathcal{U})$ is the number of holes of \mathcal{U} . The special case where Q is degenerate and $T(\mathcal{U}) = A(\mathcal{U})$ is known as the area-interaction point process, Widom–Rowlinson model, or penetrable spheres model; see, for example, [3], [15], [22], and [45].

2.2. General position of discs

It becomes essential in this paper that, with probability 1, the discs defined by Ψ are in general position in the following sense. Identify \mathbb{R}^2 with the hyperplane of \mathbb{R}^3 spanned by the first two coordinate axes. For each disc $b(z, r)$, define the *ghost sphere* $s(z, r) = \{y \in \mathbb{R}^3 : \|y - z\| = r\}$, i.e. the hypersphere in \mathbb{R}^3 with center z and radius r . A configuration of discs is said to be in *general position* if the intersection of any $k + 1$ corresponding ghost spheres is either empty or a sphere of dimension $2 - k$, where $k = 1, 2, \dots$. Note that the intersection is assumed to be empty if $k > 2$ and a sphere of dimension 0 is assumed to consist of two points. Figure 1(a) shows a configuration of discs in general position; we shall use this as a running example to illustrate forthcoming definitions.

Lemma 1. *For almost all realizations of $\Psi = \{x_1, x_2, \dots\}$, the discs $b_1 = b(x_1)$ and $b_2 = b(x_2), \dots$ are in general position.*

Proof. By Campbell’s theorem (see, for example, [41]), the mean number of sets of $k + 1$ ghost spheres whose intersection is neither empty nor of dimension $2 - k$ is given by

$$\begin{aligned}
 &\int_{\mathbb{R}^2} \int_0^\infty \cdots \int_{\mathbb{R}^2} \int_0^\infty \mathbf{1}\left[\bigcap_0^k s_i \neq \emptyset, \dim\left(\bigcap_0^k s_i\right) \neq 2 - k\right] \\
 &\quad \times \frac{\prod_0^k \rho(z_i)}{(k + 1)!} dz_0 Q(dr_0) \cdots dz_k Q(dr_k),
 \end{aligned}$$

where $\mathbf{1}[\cdot]$ is the indicator function and $s_i = s(z_i, r_i)$. This integral is 0 since, for any fixed values of $r_0 > 0, \dots, r_k > 0$, the indicator function is 0 for Lebesgue almost all $(z_0, \dots, z_k) \in \mathbb{R}^{2(k+1)}$.

All point process models for discs considered in this paper have discs in general position: by Lemma 1, the discs in X with density (1) are in general position almost surely.

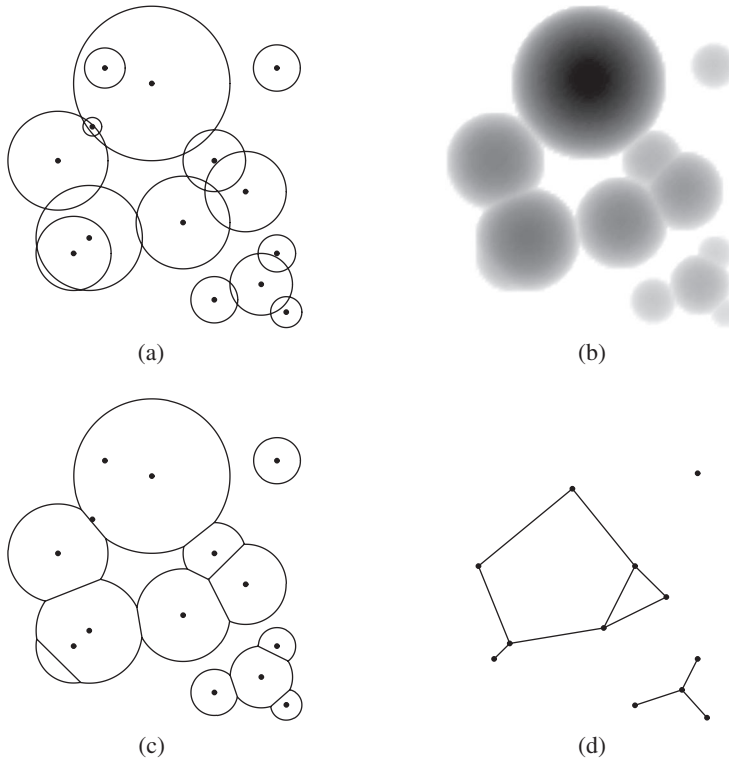


FIGURE 1: (a) A configuration of discs in general position. (b) The upper hemispheres as seen from above. (c) The power tessellation of the union of discs. (d) The dual graph.

3. Power tessellation of a union of discs

In this section we define and study the power tessellation of a union of discs

$$\mathcal{U} = \bigcup_{i \in I} b_i.$$

We assume that the discs b_i , $i \in I$, satisfy the general position assumption (GPA).

3.1. Basic definitions

In this subsection there is no need for assuming that the index set I is finite, though this will be the case in subsequent sections.

For each disc b_i , $i \in I$, with ghost sphere s_i , let $s_i^+ = \{(y_1, y_2, y_3) \in s_i : y_3 \geq 0\}$ denote the corresponding upper hypersphere and, for $u \in b_i$, let $y_i(u)$ denote the unique point on s_i^+ whose orthogonal projection on \mathbb{R}^2 is u . The subset of s_i^+ consisting of those points ‘we can see from above’ is given by

$$C_i = \{y_i(u) : u \in b_i, \|u - y_i(u)\| \geq \|u - y_j(u)\| \text{ whenever } u \in b_j, j \in I\},$$

and the GPA implies that the nonempty C_i have disjoint two-dimensional relative interiors. Thus, as illustrated in Figure 1(b), the nonempty C_i form a tessellation (i.e. subdivision) of $\bigcup_I s_i^+$ corresponding to the two-dimensional pieces of upper ghost spheres ‘as seen from

above'. Projecting this tessellation onto \mathbb{R}^2 , we obtain a tessellation of \mathcal{U} ; see Figure 1(c). Below we specify this tessellation in detail.

Let $J = \{i \in I : C_i \neq \emptyset\}$. For $i \in I$, define the *power distance* of a point $u \in \mathbb{R}^2$ from $b_i = b(z_i, r_i)$ by $\pi_i(u) = \|u - z_i\|^2 - r_i^2$, and define the *power cell* associated with b_i by

$$V_i = \{u \in \mathbb{R}^2 : \pi_i(u) \leq \pi_j(u) \text{ for all } j \in I\}.$$

For distinct $i, j \in I$, define the closed halfplane $H_{i,j} = \{u \in \mathbb{R}^2 : \pi_i(u) \leq \pi_j(u)\}$. Each V_i is a convex polygon, since it is a finite intersection of closed halfplanes $H_{i,j}$. The power cells have disjoint interiors and, by the GPA, each V_i is either empty or of dimension two. Consequently, the nonempty power cells $V_i, i \in J$, constitute a tessellation of \mathbb{R}^2 called the *power diagram* (or *Laguerre diagram*); see [1] and the references therein. In the special case where all the radii r_i are equal we have $I = J$ and the power diagram is a Voronoi tessellation (see, for example, [29] and [36]), where each cell V_i contains z_i in its interior. If the radii are not equal, a power cell V_i may not contain z_i , since $H_{i,j}$ may not contain z_i .

Let B_i denote the orthogonal projection of C_i on \mathbb{R}^2 . By Pythagoras, for all $u \in b_i$, $\pi_i(u) + \|u - y_i(u)\|^2 = 0$. Consequently, for any $i, j \in I$ and $u \in b_i \cap b_j$,

$$\|u - y_i(u)\| \geq \|u - y_j(u)\| \quad \text{if and only if} \quad \pi_i(u) \leq \pi_j(u).$$

Thus, $B_i = V_i \cap b_i$. By the GPA and the one-to-one correspondence between B_i and C_i , the collection of sets $B_i, i \in J$, constitutes a subdivision of \mathcal{U} into two-dimensional convex sets with disjoint interiors. We call this the *power tessellation of the union of discs* and denote it by \mathcal{B} . Furthermore, if $i \in J$, we call B_i the *power cell restricted to its associated disc* b_i (clearly, $B_i = \emptyset$ if $i \in I \setminus J$). Since V_i may not contain z_i , B_i may not contain z_i ; an example of this is shown in Figure 1(c). We say that a cell B_i is *isolated* if $B_i = b_i$. This means that any disc $b_j, j \in I$, intersecting b_i is contained in b_i ; the disc b_i is therefore also said to be a circular clump (see [27] and the references therein).

It is illuminating to consider Figure 1 when making the following definitions. If the intersection $e_{i,j} = B_i \cap B_j$ between two cells of \mathcal{B} is nonempty then $e_{i,j} = [u_{i,j}, v_{i,j}]$ is a closed line segment, where $u_{i,j}$ and $v_{i,j}$ denote the endpoints, and we call $e_{i,j}$ an *interior edge* of \mathcal{B} . The vertices of \mathcal{B} are given by all endpoints of interior edges. A vertex of \mathcal{B} lying on the boundary $\partial\mathcal{U}$ is called a *boundary vertex*, and it is called an *interior vertex* otherwise. Each circular arc on \mathcal{B} defined by two successive boundary vertices is called a *boundary edge* of \mathcal{B} . The circle given by the boundary of an isolated cell of \mathcal{B} is also called a boundary edge or sometimes an *isolated boundary edge*. The connected components of $\partial\mathcal{U}$ are closed curves, and each such curve is a union of certain boundary edges which either bound a hole, in which case the curve is called an *inner boundary curve*, or bound a connected component of \mathcal{U} , in which case the curve is called an *outer boundary curve*. A generic boundary edge of \mathcal{B} is written as $[u_i, v_i]$ if $B_i \neq b_i$ (a nonisolated cell), where the index means that u_i and v_i are boundary vertices of B_i , or as ∂b_i if $B_i = b_i$. We order u_i and v_i such that $[u_i, v_i]$ is the circular arc from u_i to v_i when ∂b_i is considered anticlockwise.

By the GPA, any intersection among four cells of \mathcal{B} is empty, each interior vertex corresponds to a nonempty intersection among three cells of \mathcal{B} , and exactly three edges emerge at each vertex. Note that each isolated cell has no vertices and one edge. Each interior edge $e_{i,j}$ is contained in the *bisector* (or *power line* or *radical axis*) of b_i and b_j defined by $\partial H_{i,j} = \{u \in \mathbb{R}^d : \pi_i(u) = \pi_j(u)\}$. This is the line perpendicular to the line joining the centers of the two

discs and passing through the point

$$z_{i,j} = \frac{1}{2} \left(z_i + z_j + \frac{r_j^2 - r_i^2}{\|z_i - z_j\|^2} (z_i - z_j) \right).$$

We call $E_{i,j} \equiv \partial H_{i,j} \cap b_i = \partial H_{i,j} \cap b_j$ the *chord* of $b_i \cap b_j$. Obviously, $e_{i,j} \subseteq E_{i,j}$.

The *dual graph* \mathcal{D} to \mathcal{B} has nodes equal to the centers z_i , $i \in J$, of discs generating nonempty cells, and each edge of \mathcal{D} is given by two vertices z_i and z_j such that $e_{i,j} \neq \emptyset$. See Figure 1(d). Note that there is a one-to-one correspondence between the edges of \mathcal{D} and the interior edges of \mathcal{B} .

3.2. Construction

We construct the power tessellation of a finite union of discs by successively adding the discs one by one, keeping track of old and new edges and whether each disc generates a nonempty cell or not. The updates are local in some sense and used in the ‘birth part’ of the MCMC algorithm in Section 4.7. For details, see Section A.1.

4. Results for exponential family models

In this section we study exponential family models for the point process X as specified by the density $f(x)$ in (1), assuming that the canonical sufficient statistic $\mathbf{T}(\mathcal{U}_x)$ is a linear combination of one or more of the geometric characteristics introduced in the following paragraph. We let $\text{supp}(Q)$ denote the support of Q , let

$$\Omega = \{(z, r) \in S \times (0, \infty) : \rho(z) > 0, r \in \text{supp}(Q)\}$$

denote the support of the intensity measure of the reference Poisson process Ψ , and let \mathcal{N} denote the set of all finite subsets x (also called finite configurations) of Ω so that the discs given by x are in general position. By Lemma 1, $X \in \mathcal{N}$ with probability 1. For ease of exposition, we assume that all realizations of X are in \mathcal{N} , and set $f(x) = 0$ if $x \notin \mathcal{N}$.

We let $\mathbf{T}(x)$ be given by one or more of the following characteristics of $\mathcal{U} = \mathcal{U}_x$ if $x \in \mathcal{N}$: the area $A = A(\mathcal{U})$, the perimeter $L = L(\mathcal{U})$, the Euler–Poincaré characteristic $\chi = \chi(\mathcal{U})$, the number of isolated cells $N_{ic} = N_{ic}(\mathcal{U})$, the number of connected components $N_{cc} = N_{cc}(\mathcal{U})$, the number of holes $N_h = N_h(\mathcal{U})$, the number of boundary edges (including isolated boundary edges) $N_{be} = N_{be}(\mathcal{U})$, and the number of boundary vertices $N_{bv} = N_{bv}(\mathcal{U})$. In the general case

$$\mathbf{T} = (A, L, \chi, N_h, N_{ic}, N_{bv}) \tag{4}$$

with corresponding canonical parameter $\theta = (\theta_1, \dots, \theta_6)$, and we then call X the \mathbf{T} -interaction process. If, for example, $\theta_2 = \dots = \theta_6 = 0$, we set $\mathbf{T} = A$ and refer then to the A -interaction process. Similarly, for the L -interaction process, we have $\theta_1 = 0$ and $\theta_3 = \dots = \theta_6 = 0$, for the (A, L) -interaction process, we have $\theta_3 = \dots = \theta_6 = 0$, and so on. A quermass-interaction process [22] is the special case $\mathbf{T} = (A, L, \chi)$ and $\theta_4 = \theta_5 = \theta_6 = 0$. Note that (4) specifies $N_{cc} = \chi + N_h$ and $N_{be} = N_{ic} + N_{bv}$; cf. Lemma 2, below. Thus, a continuum random-cluster model [15], [23], [28] is the special case $\mathbf{T} = N_{cc}$, $\theta_1 = \theta_2 = \theta_5 = \theta_6 = 0$, and $\theta_3 = \theta_4$. Although natural in terms of the power diagram, we may question how useful it is to include N_{ic} and N_{bv} in (4), since in practice grains may only approximately be discs and only a digital image is observed, where the resolution makes it difficult to identify circular structures. Moreover,

the interplay of (θ_5, θ_6) with other parameters seems complicated; we return to this aspect at the end of Section 4.2.

4.1. Exponential family structure

Let

$$\Theta = \left\{ (\theta_1, \dots, \theta_6) \in \mathbb{R}^6 : \int \exp(\pi\theta_1 r^2 + 2\pi\theta_2 r) Q(dr) < \infty \right\}. \tag{5}$$

Note that $(-\infty, 0]^2 \times \mathbb{R}^4 \subseteq \Theta$ and that $\Theta = \mathbb{R}^6$ if $\text{supp}(Q)$ is bounded. The following proposition states that, under a weak condition on (S, ρ, Q) , the exponential family density has Θ as its full parameter space and T in (4) as its minimal canonical sufficient statistic (for details on exponential family properties, see [5]).

Proposition 1. *Suppose that S contains a set $D = b(u, R_1) \setminus b(u, R_2)$, where $\infty > R_1 > R_2 > 0$, $\rho(z) > 0$ for all $z \in D$, and $Q((0, R_2]) > 0$. Then the point process densities*

$$f_{\theta}(x) = \frac{1}{c_{\theta}} \exp(\theta_1 A(\mathcal{U}_x) + \theta_2 L(\mathcal{U}_x) + \theta_3 \chi(\mathcal{U}_x) + \theta_4 N_h(\mathcal{U}_x) + \theta_5 N_{ic}(\mathcal{U}_x) + \theta_6 N_{bv}(\mathcal{U}_x)) \tag{6}$$

with $x \in \mathcal{N}$ and $\theta = (\theta_1, \dots, \theta_6) \in \Theta$ constitute a regular exponential family model.

Proof. Recall that an exponential family model is regular if it is full and of minimal form [5]. Later in Proposition 6, we verify that f_{θ} is well defined if and only if $\theta \in \Theta$, so the model is full. Let Ψ_S denote the restriction of Ψ to $S \times (0, \infty)$. Since $\Theta \supseteq (-\infty, 0]^2 \times \mathbb{R}^4$ is of full dimension 6 and since there is a one-to-one linear correspondence between T in (4) and $(A, L, N_{cc}, N_{ic}, N_{bv}, N_h)$, the model is on minimal form if the statistics $A, L, N_{ic}, N_{cc}, N_{bv}$, and N_h are affinely independent with probability 1 with respect to Ψ_S (see [5]). In other words, the model is on minimal form if, for any $(\alpha_0, \dots, \alpha_6) \in \mathbb{R}^7$, with probability 1,

$$\alpha_1 A(\mathcal{U}_{\Psi_S}) + \alpha_2 L(\mathcal{U}_{\Psi_S}) + \alpha_3 N_{ic}(\mathcal{U}_{\Psi_S}) + \alpha_4 N_{cc}(\mathcal{U}_{\Psi_S}) + \alpha_5 N_{bv}(\mathcal{U}_{\Psi_S}) + \alpha_6 N_h(\mathcal{U}_{\Psi_S}) = \alpha_0 \implies \alpha_0 = \dots = \alpha_6 = 0. \tag{7}$$

We verify this, using the condition on (S, ρ, Q) imposed in the proposition, and considering realizations of Ψ_S as described below, where these realizations consist of configurations of discs with centers in D and radius less than or equal to R_2 . For such configurations, given by either one disc, two nonoverlapping discs, or two overlapping discs, and if $\alpha_5 = \alpha_6 = 0$, we immediately obtain (7). Extending this to situations where only $\alpha_6 = 0$ and where we have three discs with pairwise overlap but no common intersection, we also immediately obtain (7) and the set consisting of such configurations where $N_h(\mathcal{U}_{\Psi_S}) = 0$ has a positive probability. The condition on (S, ρ, Q) also allows us, with a positive probability, to construct a set of realizations where $N_h(\mathcal{U}_{\Psi_S}) = 1$, namely by considering sequences of discs which only overlap pairwise and which form a single connected component. Thereby, for any $(\alpha_0, \dots, \alpha_6) \in \mathbb{R}^7$, with probability 1, (7) is seen to hold.

4.2. Interpretation of parameters

In this subsection we discuss the meaning of the parameters $\theta_1, \dots, \theta_6$ in the T -interaction process, (6).

We first recall the definition of the *Papangelou conditional intensity* $\lambda(x, v)$ for a general finite point process $X \subset S \times (0, \infty)$ with a hereditary density f with respect to the distribution of Ψ (see [34] and the references therein). For all finite configurations $x \subset S \times (0, \infty)$ and all discs $v = (z, r) \in S \times (0, \infty) \setminus x$, the hereditary condition means that $f(x) > 0$ whenever $f(x \cup \{v\}) > 0$, and, by definition,

$$\lambda(x, v) = \begin{cases} \frac{f(x \cup \{v\})}{f(x)} & \text{if } f(x) > 0, \\ 0 & \text{otherwise.} \end{cases}$$

This is in a one-to-one correspondence with the density f , and has the interpretation that $\lambda(x, v)\rho(z) dz Q(dr)$ is the conditional probability of X having a disc with center in an infinitesimal region containing z and of size dz and radius in an infinitesimal region containing r and of size dr , given that the rest of X is x .

For functionals $W = A, L, \dots$, define $W(x, v) = W(\mathcal{U}_{x \cup \{v\}}) - W(\mathcal{U}_x)$. The T -interaction process, (6), has a hereditary density with Papangelou conditional intensity

$$\lambda_\theta(x, v) = \exp(\theta_1 A(x, v) + \theta_2 L(x, v) + \theta_3 \chi(x, v) + \theta_4 N_h(x, v) + \theta_5 N_{ic}(x, v) + \theta_6 N_{bv}(x, v)) \tag{8}$$

if $x \cup \{v\} \in \mathcal{N}$, and $\lambda_\theta(x, v) = 0$ otherwise. Note that \mathcal{N} is hereditary, meaning that $x \in \mathcal{N}$ implies that $y \in \mathcal{N}$ if $y \subset x$. The process X is said to be *attractive* if

$$\lambda_\theta(x, v) \geq \lambda_\theta(y, v) \quad \text{whenever } y \subset x \text{ and } x \in \mathcal{N} \tag{9}$$

and *repulsive* if

$$\lambda_\theta(x, v) \leq \lambda_\theta(y, v) \quad \text{whenever } y \subset x \text{ and } x \in \mathcal{N}. \tag{10}$$

Note that, since quermass integrals are additive,

$$\begin{aligned} A(x, v) &= A(b_v) - A(b_v \cap \mathcal{U}_x), & L(x, v) &= L(b_v) - L(b_v \cap \mathcal{U}_x), \\ \chi(x, v) &= 1 - N_h(b_v \cap \mathcal{U}_x). \end{aligned} \tag{11}$$

Proposition 2. *The following assertions hold:*

- (a) *the A-interaction process is attractive if $\theta_1 < 0$ and repulsive if $\theta_1 > 0$;*
- (b) *under weak conditions, for example, if S contains an open disc, the L-interaction process is neither attractive nor repulsive if $\theta_2 \neq 0$;*
- (c) *under other weak conditions, basically meaning that S is not too small compared to $\inf \text{supp}(Q)$ (as exemplified in the proof), the W-interaction processes with $W = \chi, N_h, N_{ic}, N_{bv}$ are neither attractive nor repulsive if $\theta_i \neq 0, i = 3, 4, 5, 6$;*
- (d) *under similar weak conditions as in (c), the continuum random-cluster model (i.e. the N_{cc} -interaction process, where $\theta_3 = \theta_4$ and $\theta_1 = \theta_2 = \theta_5 = \theta_6 = 0$) is neither attractive nor repulsive if $\theta_3 \neq 0$.*

Proof. From (11), part (a) follows immediately, which is a well-known result [3]. We have $L(b_v \cap \mathcal{U}_{x_1}) > 0 = L(b_v \cap \mathcal{U}_\emptyset)$ if $b_v \cap b_{x_1} \neq \emptyset$. This provides a simple example where $\lambda_{\theta_2}(x, v)$ is decreasing or increasing in x if $\theta_2 > 0$ or $\theta_2 < 0$, respectively. On the other hand, if S contains an open disc, we may obtain the opposite case. Figure 2(a) shows such an example,

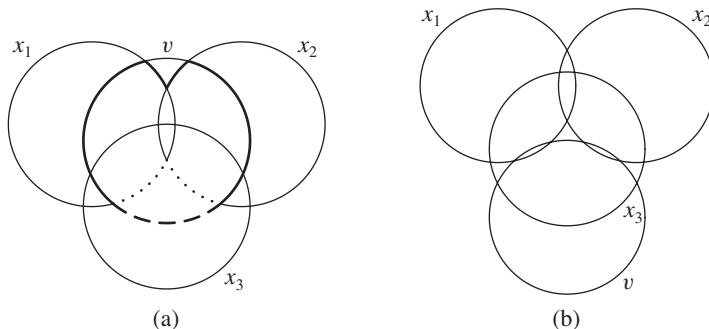


FIGURE 2: Examples of four discs of equal radii. (a) When we add x_3 to $\{x_1, x_2\}$, the dotted arcs disappear and the dashed arc appears, so $L(b_v \cap \mathcal{U}_{\{x_1, x_2, x_3\}}) < L(b_v \cap \mathcal{U}_{\{x_1, x_2\}})$. (b) $N_{b_v}(\{x_1, x_2\}, v) = 4$ and $N_{b_v}(\{x_1, x_2, x_3\}, v) = 2$.

with four discs of equal radii, where the four centers of the discs can be made arbitrarily close and where $L(b_v \cap \mathcal{U}_{x_1, x_2, x_3}) < L(b_v \cap \mathcal{U}_{x_1, x_2})$. Thereby part (b) is verified.

To verify parts (c) and (d), we again consider discs $b_v, b_{x_1}, b_{x_2}, \dots$ of equal radii, since it may be possible that Q is degenerate.

Suppose that $b_v \cap b_{x_1} = \emptyset, b_v \cap b_{x_2} \neq \emptyset$, and $b_{x_1} \cap b_{x_2} \neq \emptyset$, and let $x = \{x_1, x_2\}$. Then $\chi(y, v) = 2$ and $\chi(x, v) = 1$ if $y = \{x_1\}$, while $\chi(y, v) = 1$ and $\chi(x, v) = 2$ if $y = \{x_2\}$. Since $\chi = N_{cc}$ in these examples, we obtain part (c) in the case of the χ -interaction process and part (d) in the case of the N_{cc} -interaction process.

Suppose that b_v, b_{x_1} , and b_{x_2} have no common intersection, but that each pair of discs are overlapping, i.e. they form a hole. If $y = \{x_1, x_2\}$ and the hole disappears when we consider $x = \{x_1, x_2, x_3\}$ then $N_h(y, v) = 1$ and $N_h(x, v) = 0$. Note that $N_{b_v}(y, v) = 4$ and it may be possible that $N_{b_v}(x, v) = 2$, as exemplified in Figure 2(b). On the other hand, if $y = \{x_1\}$ and $x = \{x_1, x_2\}$ then $N_h(y, v) = 0, N_h(x, v) = 1, N_{b_v}(y, v) = 2$, and $N_{b_v}(x, v) = 4$. Hence, we have established part (c) in the case of the N_h -interaction and N_{b_v} -interaction processes.

Finally, the case of the N_{ic} -interaction process in part (c) follows simply by considering two overlapping discs and two disjoint discs.

Thus, in terms of the ‘local characteristic’ $\lambda_\theta(x, v)$, we can easily interpret the importance of the parameter θ_1 in the A -interaction process and also that of θ_2 in the L -interaction process provided that Q is degenerate, while the role of the parameters in the other processes is less clear. Their meaning is better understood in ‘global terms’ and by simulation studies. In comparison with the reference Poisson process, the A -interaction processes with $\theta_1 > 0$ and $\theta_1 < 0$ tend to produce realizations with a larger and smaller area $A(\mathcal{U}_x)$, respectively; see Figure 3(b) and (c), and similarly for the W -interaction process with $W = L, \chi, N_h, N_{ic}, N_{b_v}, N_{cc}$. For models with two or more parameters, the interpretation is more complicated and depends not only on the signs of the parameters but also on how large the parameters are, and it is, for example, possible to obtain rather similar realizations for different combinations of the parameters. See Figures 5–8 in our research report [31]. As an illustration, Figure 3(d)–(f) show realizations of the (A, L, N_{cc}) -interaction process with $(\theta_1, \theta_2) = (0.6, -1)$ and different positive values of $\theta_3 = \theta_4$. Here the effect of increasing $\theta_3 = \theta_4$ should be clear and, at least with respect to the characteristic A , the process corresponding to Figure 3(e) seems to have some similarity to the A -interaction process corresponding to Figure 3(c), although the sign of θ_1 is different in the two processes and the connected components in the two realizations look very different.

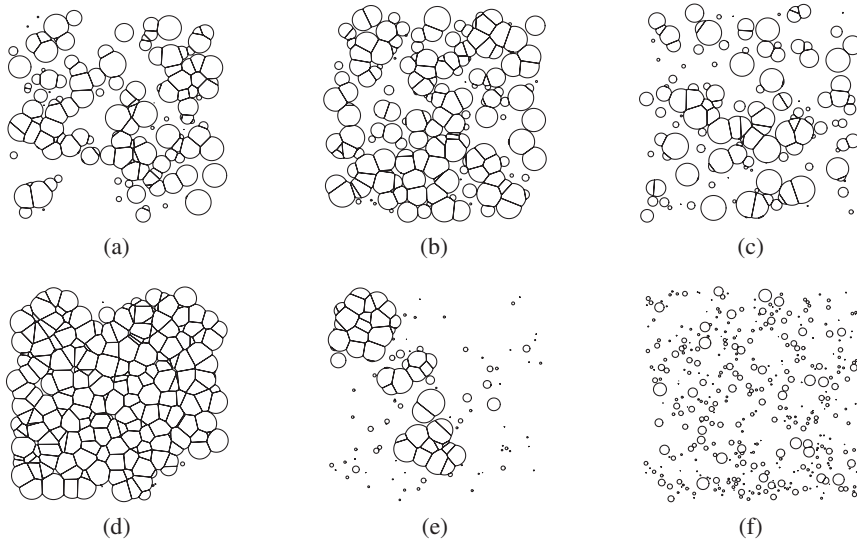


FIGURE 3: (a) The power tessellation of a realization of the reference Poisson process with Q the uniform distribution on the interval $[0, 2]$, $\rho(u) = 0.2$ on a rectangular region $S = [0, 30] \times [0, 30]$, and $\rho(u) = 0$ outside S ; simulated realizations of the A -interaction process with (b) $\theta_1 = 0.1$ or (c) $\theta_1 = -0.1$; and simulated realizations of the (A, L, N_{cc}) -interaction process with $(\theta_1, \theta_2) = (0.6, -1)$ and (d) $\theta_3 = \theta_4 = 1$, (e) $\theta_3 = \theta_4 = 2$, or (f) $\theta_3 = \theta_4 = 5$.

4.3. Geometric characteristics and inclusion–exclusion formulae

Lemmas 2 and 3, below, concern various useful relations between certain geometric characteristics of the union $\mathcal{U} = \mathcal{U}_x$ and of its power tessellation $\mathcal{B} = \mathcal{B}_x$, assuming that $x \in \mathcal{N}$. Among other things, the results become useful in connection to the computation of geometric characteristics in Section 4.4 and for the sequential constructions considered in Sections 3.2 and 4.7 and Appendix A.

Define the following characteristics of $\mathcal{B} = \mathcal{B}_x$: the number of nonempty cells $N_c = N_c(\mathcal{B})$, the number of interior edges $N_{ie} = N_{ie}(\mathcal{B})$, the number of edges $N_e = N_{be} + N_{ie}$, the number of interior vertices $N_{iv} = N_{iv}(\mathcal{B})$, and the number of vertices $N_v = N_{bv} + N_{iv}$. These statistics do not appear in the specification, (4), since they cannot be determined from \mathcal{U} ; they can be determined only from \mathcal{B} . Furthermore, let $N = n(x)$ denote the number of discs.

Lemma 2. *We have*

$$N_{ic} \leq N_{cc} \leq N_c \leq N, \quad N_{bv} = 2N_{ie} - 3N_{iv}, \tag{12}$$

and

$$\chi = N_{cc} - N_h = N_c - N_{ie} + N_{iv}. \tag{13}$$

If $N_c \geq 2$ and $N_{cc} = 1$ then

$$N_{be} = N_{bv} \leq 2N_{ie}, \quad 3N_v = 2N_e. \tag{14}$$

If $N_c \geq 3$ and $N_{cc} = 1$ then

$$N_{ie} \leq 3N_c - 6. \tag{15}$$

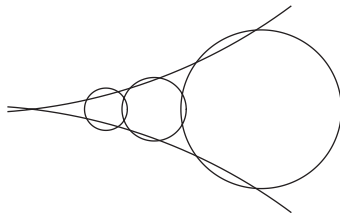


FIGURE 4: A configuration of five discs with exactly $2N_c - 5$ holes.

Moreover,

$$N_{bv} \leq 6N \tag{16}$$

and

$$N_h = 0 \text{ if } N_c \leq 2, \quad N_h \leq 2N_c - 5 \text{ if } N_c \geq 3. \tag{17}$$

Proof. The inequalities in (12) clearly hold, and the identity in (12) follows from a simple counting argument, using the facts that each interior edge has two endpoints and that exactly three interior edges emerge at each interior vertex.

The first identity in (13) is just the definition (3), and the second identity follows from Euler’s formula.

Assuming that $N_c \geq 2$ and $N_{cc} = 1$, (14) follows from simple counting arguments, using firstly the fact that exactly two boundary edges emerge at each boundary vertex, secondly the simple fact that $N_{bv} \leq N_v$, and thirdly the fact that exactly three edges emerge at each vertex.

To verify (15), consider the dual graph \mathcal{D} . Since we assume that $N_c \geq 3$ and $N_{cc} = 1$, \mathcal{D} has N_{ie} edges and N_c vertices, and so, by planar graph theory [46], since \mathcal{D} is a connected graph without multiple edges, the number of dual edges is bounded by $3N_c - 6$.

To verify (16), note that $N_{bv} \leq 2N_{ie}$; cf. (12). Using (15) and considering a sum over all components, we find that N_{ie} is bounded above by the number of components with two cells plus three times the number of components with three or more cells. Consequently, $N_{bv} \leq 6N$.

Finally, to verify (17), note that N_h is given by the sum of the number of holes of all connected components of \mathcal{U} , and a connected component consisting of one or two power cells has no holes, so it suffices to consider the case where $N_{cc} = 1$ and $N_c \geq 3$. Then, by (13), N_h is bounded above by $1 - (N_c - N_{ie})$, which in turn, by (15), is bounded above by $2N_c - 5$.

Equation (17) is a main result in [22]. Our proof of (17) is much simpler and shorter, demonstrating the usefulness of the power tessellation and its dual graph. The upper bound in (17) can be obtained for any three or more discs. If x consists of three discs b_1, b_2 , and b_3 such that $b_i \cap b_j \neq \emptyset$ for $1 \leq i < j \leq 3$ and $b_1 \cap b_2 \cap b_3 = \emptyset$, then $N_h = 1$ and $N_c = 3$, so $N_h = 2N_c - 5$. Furthermore, we may add a fourth, fifth, . . . disc, where each added disc generates two new holes—as illustrated in Figure 4 in the case of five discs—whereby $N_c = 3, 4, \dots$ and $N_h = 2N_c - 5$ in each case.

Kendall *et al.* [22] noticed the following inclusion–exclusion formula for the functionals $W = A, L, \chi$:

$$W(\mathcal{U}_x) = \sum_1^n W(b_i) - \sum_{1 \leq i < j \leq n} W(b_i \cap b_j) + \dots + (-1)^{n-1} W(b_1 \cap \dots \cap b_n), \tag{18}$$

where the sums involve $2^n - 1$ terms. Using the power tessellation, inclusion–exclusion formulae with much fewer terms are given by (12) and (13) for χ and N_{bv} and, by Lemma 3,

below, for A and L . In Lemma 3, $I_1(x)$, $I_2(x)$, and $I_3(x)$ denote index sets corresponding to nonempty cells, interior edges, and interior vertices of \mathcal{B}_x , respectively. For later use in Section 4.5, note that $I_1(x)$ and $I_2(x)$ correspond to the cliques in the dual graph \mathcal{D}_x consisting of 1 and 2 nodes, respectively, while $I_3(x)$ corresponds to the subset of 3-cliques $\{i, j, k\} \in \mathcal{D}_x$ with $b_i \cap b_j \cap b_k \neq \emptyset$ (i.e. $b_i \cup b_j \cup b_k$ has no hole). Note that if $\{i, j, k\} \in \mathcal{D}_x$ then $b_i \cap b_j \cap b_k \neq \emptyset$ if and only if $E_{i,j} \cap E_{i,k} \neq \emptyset$, where the latter property is easily checked.

Lemma 3. *The following inclusion–exclusion formulae hold for the area and perimeter of the union of discs:*

$$A(\mathcal{U}_x) = \sum_{i \in I_1(x)} A(b_i) - \sum_{\{i,j\} \in I_2(x)} A(b_i \cap b_j) + \sum_{\{i,j,k\} \in I_3(x)} A(b_i \cap b_j \cap b_k) \tag{19}$$

$$= \sum_{i \in I_1(x)} A(B_i) \tag{20}$$

and

$$L(\mathcal{U}_x) = \sum_{i \in I_1(x)} L(b_i) - \sum_{\{i,j\} \in I_2(x)} L(b_i \cap b_j) + \sum_{\{i,j,k\} \in I_3(x)} L(b_i \cap b_j \cap b_k) \tag{21}$$

$$= \sum_{e \text{ boundary edge of } \mathcal{B}_x} L(e). \tag{22}$$

Proof. Equations (19) and (21) are due to Theorem 6.2 of [10], while (20) and (22) follow immediately.

Edelsbrunner [10] established extensions to \mathbb{R}^d of the inclusion–exclusion formulae given by the second identities in (12), (19), and (21). Note that we cannot replace the sums in (19) by sums over all discs, pairs of discs, and triplets of discs from x .

4.4. Local calculations

For calculating the area and perimeter, the inclusion–exclusion formulae (20) and (22) appear to be more suited than (19) and (21) when the computations are done in combination with the sequential constructions considered in Sections 3.2 and 4.7 and Appendix A. Note that we need only do ‘local computations’.

For example, suppose that we are given the power tessellation \mathcal{B}^{old} of $\mathcal{U}^{\text{old}} = \bigcup_1^{n-1} b_i$ and that we add a new disc b_n . When constructing the new power tessellation \mathcal{B}^{new} of $\mathcal{U}^{\text{new}} = \bigcup_1^n b_i$, we need only consider the new set B_n and the old cells in \mathcal{B}^{old} which are neighbors to B_n with respect to the dual graph of \mathcal{B}^{new} (see Section A.1). Similarly, when a disc is deleted and the new tessellation is constructed, we need only do local computations with respect to the discs intersecting the disc which is deleted (see Section A.2); we study this neighbor relation given by overlapping discs in Section 4.5. Moreover, local computations are only needed when calculating N_{ic} and N_{bv} .

In order to calculate (χ, N_h) or, equivalently, (N_{cc}, N_h) , we could keep track on the inner and outer boundary curves in our sequential constructions, using a clockwise and anticlockwise orientation for the two different types of boundary curves. However, in our MCMC simulation codes, we found it easier to keep track on N_c, N_{ie}, N_{iv} , and N_{cc} , and thereby obtain χ by the second equality in (13) and, hence, obtain N_h by the first inequality in (13). In either case this is another kind of local computation, where the relevant neighbor relation is the connected component relation studied in Section 4.5.

Finally, let us explain in more detail how we can find the area A . We can easily determine the total area of all isolated cells of \mathcal{B} . Suppose that B_i is a nonempty, nonisolated cell of \mathcal{B} . Let c_i denote the arithmetic average of the vertices of B_i . Then $c_i \in B_i$, since B_i is convex. For any three points $c, u, v \in \mathbb{R}^2$, let $\Delta(c, u, v)$ denote the triangle with vertices c, u , and v . If $[u, v]$ is a boundary edge of B_i , let $\Gamma(u, v)$ denote the cap of b_i bounded by the arc $[u, v]$ and the line segment $[u, v]$. Then the area of B_i is the sum of areas of all triangles $\Delta(c_i, u, v)$, where u and v are defining an (interior or boundary) edge of B_i , plus the sum of areas of all caps $\Gamma(u, v)$, where u and v are defining a boundary edge of B_i .

4.5. Markov properties

The various Markov point process models considered in this subsection are either specified by a local Markov property in terms of the Papangelou conditional intensity or by a particular form of the density given by a Hammersley–Clifford-type theorem [2], [38]. In particular, we show that it is useful to view the T -interaction process (6) as a connected component Markov point process, where we show how a spatial Markov property becomes useful for handling edge effects. Throughout Sections 4.5.1–4.5.5, we let $x \in \mathcal{N}$.

4.5.1. *Local Markov property in terms of the overlap relation.* Consider the overlap relation ‘ \sim ’ defined on $S \times (0, \infty)$ by $u \sim v$ if and only if $b(u) \cap b(v) \neq \emptyset$. The T -interaction process is said to be Markov with respect to the overlap relation if $\lambda_\theta(x, v)$ depends only on x through $\{u \in x : u \sim v\}$, i.e. the neighbors in x to v [2], [38], [42]. Kendall *et al.* [22] observed that the quermass-interaction process is Markov with respect to the overlap relation. The following proposition generalizes this result.

Proposition 3. *The T -interaction process with density (6) is Markov with respect to the overlap relation if and only if $\theta_4 = \theta_5 = 0$.*

Proof. In other words, with respect to the overlap relation, we have to verify that the A -interaction, L -interaction, χ -interaction, and N_{bv} -interaction processes are Markov, while the N_h -interaction and N_{ic} -interaction processes are not Markov. It follows immediately from (8) and (11) that the A -interaction, L -interaction, and χ -interaction processes are Markov, and Figures 5 and 6 respectively show that the N_h -interaction and N_{ic} -interaction processes are not Markov. If w is a boundary vertex of \mathcal{U}_x but not of $\mathcal{U}_{x \cup \{v\}}$ then w is contained in the disc v . If instead w is a boundary vertex of $\mathcal{U}_{x \cup \{v\}}$ but not of \mathcal{U}_x then w is given by the intersection of the boundaries of v and an x -disc. Consequently, $N_{bv}(x, v) = N_{bv}(\mathcal{U}_{x \cup \{v\}}) - N_{bv}(\mathcal{U}_x)$ depends on x only through $\{u \in x : u \sim v\}$, so the N_{bv} -interaction process is Markov. This completes the proof.

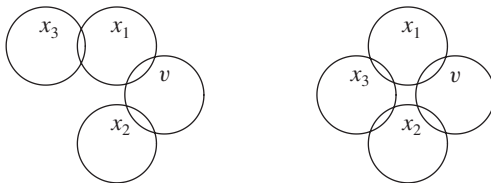


FIGURE 5: An example showing that the N_h -interaction process is not Markov with respect to the overlap relation: both $N_h(x, v) = 0$ (left) and $N_h(x, v) = 1$ (right) depend on the disc x_3 , which is not overlapping the disc v .

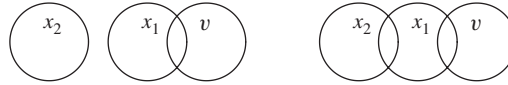


FIGURE 6: An example showing that the N_{ic} -interaction process is not Markov with respect to the overlap relation: both $N_{ic}(x, v) = -1$ (left) and $N_{ic}(x, v) = 0$ (right) depend on the disc x_2 , which is not overlapping the disc v .

As noted in [22], using the inclusion–exclusion formula (18), the Hammersley–Clifford representation [38] of the quermass–interaction process is

$$f_{(\theta_1, \theta_2, \theta_3)}(x) = \prod_{y \subseteq x} \phi_{(\theta_1, \theta_2, \theta_3)}(y), \tag{23}$$

where the interaction function is given by

$$\phi_{(\theta_1, \theta_2, \theta_3)}(x) = \exp\left((-1)^n \left(\theta_1 A \left(\bigcap_1^n b_i \right) + \theta_2 L \left(\bigcap_1^n b_i \right) + \theta_3 \chi \left(\bigcap_1^n b_i \right) \right)\right) \tag{24}$$

for nonempty $x = \{(z_1, r_1), \dots, (z_n, r_n)\}$ and $\phi_{(\theta_1, \theta_2, \theta_3)}(\emptyset) = 1/c_{(\theta_1, \theta_2, \theta_3)}$. However, for at least two reasons, it is the density in (6) of the quermass–interaction process rather than the Hammersley–Clifford representation (23) which seems appealing. First, the process has interactions of all orders, since $\log \phi_{(\theta_1, \theta_2, \theta_3)}(x)$ can be nonzero no matter how many discs x are specified by X , so the calculation of the interaction function (24) can be very time consuming. Second, (23) does not seem to be of much relevance if we can observe \mathcal{U}_X but not X . This indicates that another kind of neighbor relation is needed when describing the Markov properties. Two other relations are therefore discussed below.

4.5.2. *Local Markov property in terms of the dual graph.* It is natural to ask whether T -interaction processes in the sense of [2] are nearest-neighbor Markov point processes with respect to the neighbor relation defined by the dual graph. Below we show that this is not the case in general.

First consider the case of the quermass–interaction process. Applying the inclusion–exclusion formulae given by the last identity in (13), (19), and (21), we obtain another representation of the quermass–interaction process density, namely as a product of terms corresponding to the cliques in the dual graph, excluding the following case of 3-cliques $\{i, j, k\} \in \mathcal{D}_x$ with $b_i \cap b_j \cap b_k = \emptyset$:

$$\begin{aligned} f_{(\theta_1, \theta_2, \theta_3)}(x) &= \frac{1}{c_{(\theta_1, \theta_2, \theta_3)}} \prod_{i \in I_1(x)} \phi_{(\theta_1, \theta_2, \theta_3)}(x_i) \prod_{\{i, j\} \in I_2(x)} \phi_{(\theta_1, \theta_2, \theta_3)}(\{x_i, x_j\}) \\ &\quad \times \prod_{\{i, j, k\} \in I_3(x)} \phi_{(\theta_1, \theta_2, \theta_3)}(\{x_i, x_j, x_k\}), \end{aligned} \tag{25}$$

where now

$$\begin{aligned} \phi_{(\theta_1, \theta_2, \theta_3)}(x_i) &= \exp(\theta_1 A(b_i) + \theta_2 L(b_i) + \theta_3), \\ \phi_{(\theta_1, \theta_2, \theta_3)}(\{x_i, x_j\}) &= \exp(-\theta_1 A(b_i \cap b_j) - \theta_2 L(b_i \cap b_j) - \theta_3), \\ \phi_{(\theta_1, \theta_2, \theta_3)}(\{x_i, x_j, x_k\}) &= \exp(\theta_1 A(b_i \cap b_j \cap b_k) + \theta_2 L(b_i \cap b_j \cap b_k) + \theta_3). \end{aligned}$$

This is of a somewhat similar form to the Hammersley–Clifford representation for a nearest-neighbor Markov point process with respect to the neighbor relation defined by the dual graph; however, it is not exactly of the required form, since in (25) we do not have a product over all $u \in x$ but a product only over those u generating nonempty cells in \mathcal{B}_x . More precisely, since it can be verified that this neighbor relation satisfies certain consistency conditions, the quermass-interaction process is not a nearest-neighbor Markov point process with respect to the dual graph (Theorem 4.13 of [2]).

Next, we do not expect the N_h -interaction and N_{ic} -interaction processes to be nearest-neighbor Markov point processes with respect to the dual graph, since we have again been unable to obtain a Hammersley–Clifford representation.

In contrast, the N_{bv} -interaction process is a nearest-neighbor Markov point process with respect to the dual graph, since the identity in (12) implies the Hammersley–Clifford representation,

$$f_{\theta_6}(x) = \frac{1}{c_{\theta_6}} \prod_{\{i,j\} \in I_2(x)} \exp(2\theta_6) \prod_{\{i,j,k\} \in I_3(x)} \exp(-3\theta_6). \tag{26}$$

Note that (25) and (26) do not seem to be of much relevance if we can observe \mathcal{U}_X but not X .

4.5.3. Local Markov property in terms of the connected components. In our opinion, the most relevant results are Propositions 4 and 5, below, where the first proposition states that X is a connected component Markov point process [2], [4], [7], [30] and the second proposition specifies a spatial Markov property. As explained in further detail in [2], for a connected component Markov point process, the Papangelou conditional intensity depends only on local information with respect to the connected component relation ‘ \sim_x ’ defined as follows: for $u, v \in x, u \sim_x v$ if and only if $b(u)$ and $b(v)$ are contained in the same connected component K of \mathcal{U}_x . Thereby MCMC computations become ‘local’, as discussed further in Section 4.7. The spatial Markov property is discussed in Sections 4.5.4 and 4.5.5.

Proposition 4. *The T -interaction process with density (6) is a connected component Markov point process.*

Proof. The density is of the form

$$\frac{1}{c_{\theta}} \prod_{K \in \mathcal{K}(\mathcal{U}_x)} \exp(\theta_1 A(K) + \theta_2 L(K) + \theta_3 \chi(K) + \theta_4 N_h(K) + \theta_5 N_{ic}(K) + \theta_6 N_{bv}(K)), \tag{27}$$

where $\mathcal{K}(\mathcal{U}_x)$ is the set of connected components of \mathcal{U}_x . Thus, by Lemma 1 of [4], it is a connected component Markov point process.

In the discrete case (discs replaced by pixels) a Markov connected component field [33], which is also assumed to be a second-order Markov random field, has a density of a similar form as (27).

4.5.4. Spatial Markov property in terms of the overlap relation. Consider again the quermass-interaction process and, for the moment, assume that $R = \text{supp}(Q) < \infty$. Let $W_{\ominus 2R} = \{u \in W : b(u, 2R) \subseteq W\}$ be the $2R$ -clipped window of points in W so that almost surely no disc of X with center in $W_{\ominus 2R}$ intersects another disc of X with center in W^c , where $W^c = S \setminus W$. Split X into $X^{(1)}, X^{(2)}$, and $X^{(3)}$ corresponding to discs with centers in $W_{\ominus 2R}, W \setminus W_{\ominus 2R}$, and W^c , respectively. The spatial Markov property [38] states that $X^{(1)}$ and $X^{(3)}$ are conditionally

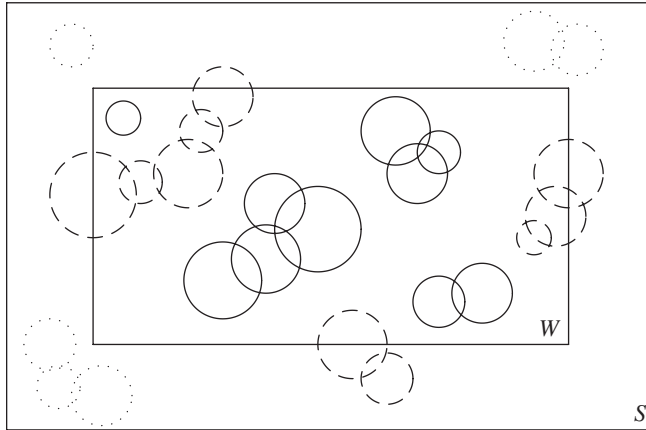


FIGURE 7: Illustrating possible realizations of $X^{(a)}$ (full circles), $X^{(b)}$ (dashed circles), and $X^{(c)}$ (dotted circles).

independent given $X^{(2)}$, and the conditional distribution $X^{(1)} \mid X^{(2)} = x^{(2)}$ has density

$$f_{\theta_1, \theta_2, \theta_3}(x^{(1)} \mid x^{(2)}) = \frac{1}{c_{\theta_1, \theta_2, \theta_3}(x^{(2)})} \exp(\theta_1 A(\mathcal{U}_{x^{(1)} \cup x^{(2)}}) + \theta_2 L(\mathcal{U}_{x^{(1)} \cup x^{(2)}}) + \theta_3 \chi(\mathcal{U}_{x^{(1)} \cup x^{(2)}})) \quad (28)$$

with respect to the reference Poisson process Ψ restricted to discs with centers in the $2R$ -clipped window. This is also a Markov point process with respect to the overlap relation restricted to $W_{\ominus 2R}$, since the Papangelou conditional intensity $\lambda_{\theta}(x^{(1)}, v \mid x^{(2)})$ corresponding to (28) is related to that in (8) by

$$\lambda_{\theta}(x^{(1)}, v \mid x^{(2)}) = \lambda_{\theta}(x^{(1)} \cup x^{(2)}, v). \quad (29)$$

However, it is problematic to use this conditional process in practice, since both (28) and (29) depend on $\mathcal{U}_{x^{(2)}} \setminus W$, which is not observable.

4.5.5. *Spatial Markov property in terms of the connected component relation.* The following spatial Markov property is more useful and applies for the general case of the T -interaction process (6), using the fact that it is a connected component Markov point process (see also [18] and [30]). We split X into $X^{(a)}$, $X^{(b)}$, and $X^{(c)}$ corresponding to discs belonging to connected components of \mathcal{U}_X which are respectively (a) contained in W , (b) intersecting both W and W^c , and (c) contained in W^c ; see Figure 7. Furthermore, let $x^{(b)}$ denote any feasible realization of $X^{(b)}$, i.e. $x^{(b)}$ is a finite configuration of discs such that K intersects both W and W^c for all $K \in \mathcal{K}(\mathcal{U}_{x^{(b)}})$.

Proposition 5. *Conditional on $X^{(b)} = x^{(b)}$, we have $X^{(a)}$ and $X^{(c)}$ are independent, and the conditional distribution of $X^{(a)}$ depends only on $x^{(b)}$ through $V = W \cap \mathcal{U}_{x^{(b)}}$ and has density*

$$f_{\theta}(x^{(a)} \mid V) = \frac{1}{c_{\theta}(V)} \mathbf{1}[\mathcal{U}_{x^{(a)}} \subseteq W \setminus V] \exp(\theta \cdot T(x^{(a)})) \quad (30)$$

with respect to the reference Poisson process of discs.

Proof. Let Π denote the distribution of Ψ restricted to those finite configurations of discs with centers in S , and let h_θ denote the unnormalized density given by the exponential term in (27). Recall the ‘Poisson expansion’ (see, for example, [34])

$$\begin{aligned} P(X \in F) &= \frac{1}{c_\theta} \int_F h_\theta(x) \Pi(dx) \\ &= \frac{1}{c_\theta} \exp\left(-\int_S \rho(u) du\right) \\ &\quad \times \sum_{n=0}^\infty \frac{1}{n!} \int_S \int \cdots \int_S \int h_\theta(x) \mathbf{1}[x \in F] \rho(u_1) du_1 Q(dr_1) \cdots \rho(u_n) du_n Q(dr_n) \end{aligned}$$

(where the term with $n = 0$ is read as 1 if the empty configuration is in the event F and 0 otherwise). From this and (27), we find that $(X^{(a)}, X^{(b)}, X^{(c)})$ has joint density

$$\begin{aligned} f(x^{(a)}, x^{(b)}, x^{(c)}) &= \frac{1}{c_\theta} \mathbf{1}[\mathcal{U}_{x^{(a)}} \subseteq W \setminus \mathcal{U}_{x^{(b)}}] h_\theta(x^{(a)}) \mathbf{1}[\mathcal{U}_{x^{(c)}} \subseteq W^c \setminus \mathcal{U}_{x^{(b)}}] h_\theta(x^{(c)}) \\ &\quad \times \mathbf{1}[\text{for all } K \in \mathcal{K}(\mathcal{U}_{x^{(b)}}): K \cap W \neq \emptyset, K \cap W^c \neq \emptyset] h_\theta(x^{(b)}) \end{aligned}$$

with respect to the product measure $\exp(2 \int_S \rho(u) du) \Pi \times \Pi \times \Pi$. Thereby the proposition follows.

The density (30) may be useful for statistical applications, since it accounts for edge effects and depends only on the union of discs intersected by the observation window W . It is a hereditary density of a connected component Markov point process with discs contained in $W \setminus V$. Its Papangelou conditional intensity $\lambda_\theta(x^{(a)}, v \mid V)$ is simply given by

$$\lambda_\theta(x^{(a)}, v \mid V) = \lambda_\theta(x^{(a)}, v) \mathbf{1}[\mathcal{U}_{x^{(a)} \cup \{v\}} \subseteq W \setminus V]. \tag{31}$$

4.6. Stability

Consider the ‘unnormalized density’ $h_\theta(x) = \exp(\theta \cdot T(x))$ corresponding to the T -interaction process with density f_θ given in (6), and recall the definition of the parameter space Θ , (5). In fact, we have not yet verified that $c_\theta \equiv E h_\theta(\Psi \cap (S \times (0, \infty)))$ is finite for $\theta \in \Theta$ and, hence, that $f_\theta = h_\theta/c_\theta$ is a well-defined density with respect to the reference Poisson process Ψ if $\theta \in \Theta$. In this subsection we discuss two stability properties which imply integrability of h_θ as well as other desirable properties.

4.6.1. Ruelle stability. This means that there exist positive constants α and β such that $h_\theta(x) \leq \alpha \beta^{n(x)}$ for all $x \in \mathcal{N}$ (in fact, this and other stability properties mentioned in this paper need only hold almost surely with respect to Ψ ; however, for ease of presentation, we shall ignore such nullsets). Ruelle stability implies that $c_\theta \leq \alpha \exp((\beta - 1) \int_S \rho(z) dz) < \infty$, and we say that $f_\theta = h_\theta/c_\theta$ is a *Ruelle stable density*. Other implications of Ruelle stability are discussed in Section 2.1 of [22] and the references therein.

The main question addressed in [22] was how to establish Ruelle stability of the quermass-interaction process, and the following proposition provides a very easy proof of this issue in connection to the general case of the T -interaction process (6) (since the proof is based on Lemma 2, the usefulness of the power tessellation is once again demonstrated).

Proposition 6. *For all $\theta \in \Theta$, $c_\theta < \infty$ and f_θ in (6) is a Ruelle stable density. If $\theta \in \mathbb{R}^6 \setminus \Theta$ then $c_\theta = \infty$.*

Proof. Note that a finite product of Ruelle stable functions is a Ruelle stable function. Let θ_0 denote a real parameter. From Lemma 2, it follows that χ, N_h, N_{ic} , and N_{bv} are bounded above by $6N$, so the functions $\exp(\theta_0 W)$, $W = \chi, N_h, N_{ic}, N_{bv}$, are Ruelle stable for all $\theta_0 \in \mathbb{R}$. Moreover, $\exp(\theta_1 A + \theta_2 L)$ is Ruelle stable if $a \equiv \int \exp(\pi\theta_1 r^2 + 2\pi\theta_2 r) Q(dr)$ is finite, since $\exp(\theta_1 A + \theta_2 L) \leq \exp((a - 1) \int_S \rho(z) dz)$. On the other hand, the first term in the infinite sum in (2) is $a \exp(\theta_3 + \theta_5) \int_S \rho(z) dz$, where $\int_S \rho(z) dz > 0$; cf. Section 2.1. Consequently, $c_\theta = \infty$ if $a = \infty$.

4.6.2. *Local stability.* This means that there exists a constant β such that, for all $x \in \mathcal{N}$ and all $v \in \Omega \setminus x$,

$$\lambda_\theta(x, v) \leq \beta. \tag{32}$$

This property is clearly implying Ruelle stability. Local stability is useful when establishing geometric ergodicity of MCMC algorithms (see [13], [34], and also Section 4.7), and it is needed in order to apply the dominating coupling from the past algorithm in [20] and [21] for making perfect simulations. Note that a finite product of locally stable functions is a locally stable function, since its Papangelou conditional intensity is given by a product of uniformly bounded Papangelou conditional intensities. The Papangelou conditional intensity (6) is a product of Papangelou conditional intensities corresponding to functions $h_{\theta_0}(x) = \exp(\theta_0 W(\mathcal{U}_x))$ with $W = A, L, \dots$ and $\theta_0 = \theta_1, \theta_2, \dots$.

As shown below, the picture of whether local stability is satisfied or not depends much on the particular type of model. In the following proposition, when we write ‘in general’, the proof of the proposition will show examples where local stability is not satisfied, depending on how S and $\text{supp}(Q)$ are specified, and it should be obvious to the reader that local stability will not be satisfied in many other cases as well. We let $\varepsilon = \inf \text{supp}(Q)$ and $R = \sup \text{supp}(Q)$.

Proposition 7. *Local stability is satisfied for*

- (a) *the A-interaction process if and only if $\theta_1 \leq 0$ or $R < \infty$;*
- (b) *the L-interaction process if $\theta_2 = 0$, or $R < \infty$ if $\theta_2 > 0$, or $\varepsilon > 0$ and $R < \infty$ if $\theta_2 < 0$; otherwise in general it is not locally stable;*
- (c) *the χ -interaction process if $\theta_3 \geq 0$, while in general it is not locally stable if $\theta_3 < 0$;*
- (d) *the N_{cc} -interaction process if $\theta_3 = \theta_4 \geq 0$ or both $\theta_3 = \theta_4 < 0$ and $\varepsilon > 0$, while it is not locally stable if $\theta_3 = \theta_4 < 0$ and $\varepsilon = 0$;*
- (e) *the N_{ic} -interaction process if $\theta_5 \geq 0$ or $\varepsilon > 0$, while it is not locally stable if $\theta_5 < 0$ and $\varepsilon = 0$.*

Moreover, local stability is in general not satisfied for

- (f) *the N_h -interaction process unless $\theta_4 = 0$;*
- (g) *the N_{bv} -interaction process unless $\theta_6 = 0$.*

Proof. Let $x \in \mathcal{N}$ and $v \in \Omega \setminus x$.

It follows from (11) that $\lambda_{\theta_1}(\emptyset, v) = \exp(\pi\theta_1 r^2)$, $\lambda_{\theta_1}(x, v) \leq \exp(\pi\theta_1 r^2)$ if $\theta_1 \geq 0$, and $\lambda_{\theta_1}(x, v) \leq 1$ if $\theta_1 \leq 0$. Thereby part (a) follows, and in a similar way we verify part (b) in the case in which $\theta_2 \geq 0$. It also follows from (11) that the χ -interaction process is locally stable if $\theta_3 \geq 0$.

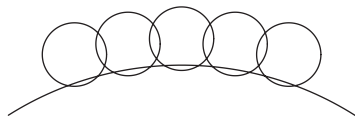


FIGURE 8: A configuration x of $n = 6$ discs intersected by another disc b_v such that $\#holes(b_v \cap \mathcal{U}_x) = n - 1 = 5$.

To verify part (b) in the case in which $\theta_2 < 0$, we first suppose that $\varepsilon > 0$ and $R < \infty$, and use an argument which Wilfrid Kendall kindly pointed out to us. A boundary edge corresponding to an angle $0 < \varphi < 2\pi$ and a disc of radius r has length φr , and it defines a sector of area $\varphi r^2/2$. Since such sectors have disjoint interiors,

$$A(\mathcal{U}_x) \geq \sum_j \frac{\varphi_j r_j^2}{2} \geq \frac{\varepsilon^2}{2} \sum_j \varphi_j,$$

where the sum is over all boundary edges. Hence,

$$L(\mathcal{U}_x) = \sum_j \varphi_j r_j \leq R \sum_j \varphi_j \leq \frac{2R}{\varepsilon^2} A(\mathcal{U}_x) < c,$$

where c is a finite constant (since the discs specified by x have centers in the bounded region S and their radii are bounded by R , $A(\mathcal{U}_x)$ has an upper bound). Consequently,

$$L(x, v) = L(b_v) - L(b_v \cap \mathcal{U}_x) \geq 2\pi\varepsilon - c,$$

and so local stability is established when $\theta_2 < 0$, $\varepsilon > 0$, and $R < \infty$.

On the other hand, suppose that $\varepsilon = 0$ or $R = \infty$. Let r denote the radius of b_v , let $0 < \delta < r$, and consider the infinite configuration of discs of radii δ and centers at the sites of an equilateral triangular lattice of side length 2δ . The proportion of \mathbb{R}^2 covered by these discs is the so-called maximal packing degree $p = \pi/\sqrt{12}$ (a number independent on how δ is chosen). Now, suppose that x is the subconfiguration of all such discs contained in b_v . As either δ decreases to 0 or r increases to ∞ , $n(x)\delta^2/r^2$ converges to p , and so

$$L(x, v) = L(b_v) - L(b_v \cap \mathcal{U}_x) = 2\pi r - 2\pi\delta n(x)$$

is converging to $-\infty$. Hence, if $\theta_2 < 0$, the local stability condition is violated, and so part (b) is verified.

To show an example where the χ -interaction process is not locally stable if $\theta_3 < 0$, consider Figure 8. Suppose that $x = \{x_1, \dots, x_n\}$ corresponds to the pairwise overlapping small discs in Figure 8 and that b_v corresponds to the large disc. Then each pair x_i, x_{i+1} together with b_v form one hole, and $N_h(b_v \cap \mathcal{U}_x) = n - 1$. Since n may be arbitrarily large, using (11) again, we obtain part (c). Note that b_v does not need to be so large compared to the other discs in Figure 8; it is only chosen in this way for illustrative purposes. For example, all the discs may be of a very similar size so that $N_h(b_v \cap \mathcal{U}_x) = n - 1$ still (then the discs in x will be much more overlapping than indicated in Figure 8). More precisely, whether this holds or not depends on how large S is compared to $\text{supp}(Q)$. For instance, if S is a disc with radius R and

$\Omega = S \times \{2R\}$ then $\chi(\mathcal{U}_x) = 1$ for all $x \in \mathcal{N}$, and so the χ -interaction process is locally stable for all $\theta_3 \in \mathbb{R}$.

For part (d), we use the fact that

$$N_{cc}(x, v) = 1 - \#\{\text{connected components in } \mathcal{U}_x \text{ which are intersected by } b_v\}. \tag{33}$$

Hence, we immediately obtain local stability if $\theta_3 = \theta_4 \geq 0$. Suppose instead that $\theta_3 = \theta_4 < 0$. By (33), $N_{cc}(x, v)$ has no lower bound if $\varepsilon = 0$, since the discs in x can be disjoint and still all intersect b_v . On the other hand, if $\varepsilon > 0$ then $1 - N_{cc}(x, v)$ is at most equal to the maximal number of disjoint discs with radius ε and centers in S . Thereby part (d) is verified. The proof of part (e) is similar, using instead the fact that

$$N_{ic}(x, v) = \mathbf{1}_{ic}(x, v) - \#\{\text{isolated cells in } \mathcal{U}_x \text{ which are contained in } b_v\},$$

where $\mathbf{1}_{ic}(x, v)$ is the indicator function which is 1 if B_v is an isolated cell in $\mathcal{B}_{x \cup \{v\}}$ and 0 otherwise.

The N_h -interaction process with $\theta_4 = 0$ and the N_{bv} -interaction process with $\theta_6 = 0$ are nothing but the Poisson process Ψ , and so local stability is obviously satisfied. By similar arguments as above in the proof of part (c), when $\theta_3 < 0$, there are in general no uniform upper and lower bounds on either $N_h(x, v)$ or $N_{bv}(x, v)$. Thereby, parts (f) and (g) follow.

Proposition 7 immediately extends to the conditional quermass-interaction process with density (28) and the conditional T -interaction process in (30). Note that if the indicator term in (30) is 1, it implies that the radius of any disc in $x^{(a)}$ is less than a constant. Consequently, (a) the conditional A -interaction process given by (30) is always locally stable, and (b) the L -interaction process given by (30) is locally stable if either $\theta_2 \geq 0$ or $\theta_2 < 0$ and $\varepsilon > 0$, and in general it is not locally stable if $\theta_2 < 0$ and $\varepsilon = 0$.

4.7. MCMC algorithms

For simulation of the T -interaction process (6), the conditional quermass-interaction point process with density (28), or the conditional T -interaction process with density (30), we use a simple version of the birth–death type Metropolis–Hastings algorithm studied in [13], [14], and [34]. For specificity, we first consider the T -interaction process X with Papangelou conditional intensity $\lambda_\theta(x, v)$ given by (8).

In the Metropolis–Hastings algorithm if x is the state at iteration t , we generate a proposal which is either a ‘birth’ $x \cup \{v\}$ of a new disc $v = (z, r)$ or a ‘death’ $x \setminus \{x_i\}$ of an old disc $x_i \in x$. Each kind of proposal may happen with equal probability $\frac{1}{2}$. Define

$$r_\theta(x, v) = \lambda_\theta(x, v) \frac{\int_S \rho(s) ds}{\rho(z)(n(x) + 1)}. \tag{34}$$

In the case of a birth proposal, v follows the normalized intensity measure of Ψ , i.e. z and r are independent, z has a density on S proportional to ρ , and r follows the mark distribution Q . This proposal is accepted as the state at iteration $t + 1$ with probability $\min\{1, H_\theta(x, v)\}$, where the Hastings ratio is given by $H_\theta(x, v) = r_\theta(x, v)$. In the case of a death proposal, x_i is a uniformly selected point from x , and the Hastings ratio in the acceptance probability of the proposal is now given by $H_\theta(x, x_i) = 1/r_\theta(x \setminus \{x_i\}, x_i)$ (in the special case where $x = \emptyset$, we do nothing). Finally, if neither kind of proposal is accepted, we retain x at iteration $t + 1$.

As verified in [14], the generated Markov chain is aperiodic and positive Harris recurrent, the chain converges towards the distribution of X , and Birkhoff’s ergodic theorem establishes

convergence of Monte Carlo estimates of mean values with respect to (6). If local stability is satisfied (see Proposition 7), the chain is geometrical ergodic and, hence, a central limit theorem applies for Monte Carlo estimates [6], [34], [39]. Moreover, from a computational perspective, the important point of the algorithm is that it only involves calculating the Papangelou conditional intensity, so only local computations of the statistics appearing in (8) are needed; cf. Sections 4.3–4.5.

In theory we may use any state of \mathcal{N} as the initial state of the algorithm, but we have mainly used three kinds of initial states:

- (i) the extreme case of the empty configuration \emptyset ;
- (ii) if local stability is satisfied, the other extreme case is given by a realization from a Poisson process Ξ with intensity measure $\beta\rho(z) dz Q(dr)$, where β is the upper bound in (32);
- (iii) a realization of the reference Poisson process Ψ (an intermediate case of (i) and (ii) if $\beta > 1$).

In fact, local stability ensures that the Poisson process in (ii) can be coupled with X so that $X \subseteq \Xi$, and this kind of domination can be exploited to make perfect simulations of X , using a dominating coupling from the past algorithm [19], [21].

The algorithm for simulating from the conditional processes with densities (28) and (30) is the same except that we replace $\lambda_\theta(x, v)$ in (34) by the Papangelou conditional intensities in (29)–(31), and that the state space has of course to be in accordance with (28) and (30). The convergence properties and computations are therefore similar to those discussed above. The initial states are of course slightly different, where we modify the Poisson process in (ii) or (iii) above as follows. For (28), we restrict the Poisson process in (ii) or (iii) so that the centers are in $W_{\ominus 2R}$. For (30), we first restrict the Poisson process in (ii) or (iii) so that the centers are in W , and second, when we make a simulation from this Poisson process, we finally omit those discs which are not included in $W \setminus V$.

5. Extensions and open problems

We conclude with some remarks on possible extensions of this work and on some open problems.

We demonstrated the usefulness of the power tessellation in connection to the T -interaction process (4), and argued why this model is best viewed as a connected component Markov point process. For the specification of the sufficient statistic T , other geometric characteristics than those in (4) may be of interest to include, for example, the shape characteristic for the connected components K such as $A(K)/L(K)^2$. The power tessellation will also be a useful tool for such extensions, not least since local calculations can be carried out as discussed in Section 4.4.

We confined ourselves to the case of discs in \mathbb{R}^2 , though many concepts and results can be extended to the general case of balls in \mathbb{R}^d . The planar case, $d = 2$, is already complicated enough, and indeed the power tessellation in higher dimensions becomes more complicated; cf. [10]. The planar case is of principal importance for applications in spatial statistics and stochastic geometry (see, e.g. [8] and [41]), and the spatial case, $d = 3$, is of particular importance in physics and computational biology (see, e.g. [11], [24], [25], and [26]).

The T -interaction processes obviously provide a large and flexible class of random models for unions of discs. It would be interesting to get a better understanding of the importance of the parameters $\theta_1, \dots, \theta_6$; cf. Section 4.2. For instance, how different are the models which have been simulated in Section 4.2 and how different would a fitted L -interaction process be if

the true model is an A -interaction process? Probably, to answer such questions, an extensive simulation study will be required.

As noted in Section 4.6, the dominating coupling from the past algorithm [20], [21] for making perfect simulations requires local stability. Moreover, to make this algorithm work in practice, some monotonicity property like (9) or an antimonotonicity property like (10) is useful, but apart from the A -interaction process, our models are in general neither attractive nor repulsive; cf. Proposition 2. How difficult is it to make a perfect simulation of, for example, the L -interaction process?

Also, extensions of our T -interaction models to infinite configurations of discs would be of interest, particularly for applications in statistical physics. Such extensions are possible for quermass-interaction models, at least if Q has bounded support (see [22]), but how do we extend the other kind of T -interaction models? The usual approach is to use a local specification in the sense of [37] or, equivalently, to specify the Papangelou conditional intensity for the infinite process [12], [35], but this would require that the connected components are almost surely bounded. See the somewhat related discussion in [33] concerning infinite extensions of Markov connected component fields.

A problem related to infinite extensions of T -interaction models is the issue of phase transition. The A -interaction model exhibits phase transition, at least if the radii are all fixed at a constant value [15], [40], but what about other T -interaction models?

Finally, we are currently exploiting the results in this paper to study the statistical aspects, in particular likelihood-based inference, in a follow up paper [32].

Appendix A. Successive construction of power tessellations

In this appendix we explain how to construct a new power tessellation of a union of discs by adding a new disc (Section A.1) or deleting an old disc (Section A.2), assuming that the old power tessellation is known. The constructions can easily be extended to keep track on the connected components of the union of discs, but to save space we omit these details.

A.1. The case where a new disc is added

Suppose that we want to construct a new power tessellation \mathcal{B}^{new} of a union $\mathcal{U}^{\text{new}} = \bigcup_1^n b_i$ of $n \geq 1$ discs in general position, where we are adding the disc b_n and we have already constructed the power tessellation \mathcal{B}^{old} of $\mathcal{U}^{\text{old}} = \bigcup_1^{n-1} b_i$ based on the $n - 1$ other discs (if $n = 1$ then \mathcal{B}^{old} and \mathcal{U}^{old} are empty). More precisely, with respect to \mathcal{B}^{old} , we assume that we know all the old edges. We denote the old interior edges by $[u_{i,j}^{\text{old}}, v_{i,j}^{\text{old}}]$ and the old boundary edges by $[u_i^{\text{old}}, v_i^{\text{old}}]$ or $\partial b_i^{\text{old}}$. We want to construct the new tessellation \mathcal{B}^{new} of $\mathcal{U}^{\text{new}} = \mathcal{U}^{\text{old}} \cup b_n$ by finding its interior edges $[u_{i,n}^{\text{new}}, v_{i,n}^{\text{new}}]$ and boundary edges $[u_n^{\text{new}}, v_n^{\text{new}}]$ associated to the new cell B_n^{new} . This is done in steps (ii) and (iv), below. Moreover, to obtain the remaining new edges, we modify old interior edges $[u_{i,j}^{\text{old}}, v_{i,j}^{\text{old}}]$ and old boundary edges $[u_i^{\text{old}}, v_i^{\text{old}}]$ or $\partial b_i^{\text{old}}$, noting that a ‘modified old edge’ can be unchanged, reduced, or disappearing. This is done in steps (iii) and (v), below. Note that steps (i), (ii), and (iv) determine the new cells, i.e. which of the sets $B_1^{\text{new}}, \dots, B_n^{\text{new}}$ are empty or not.

(i) *Considering old discs intersecting the new disc.* If b_n is contained in some disc b_j with $j < n$ then B_n^{new} is empty and so $\mathcal{B}^{\text{new}} = \mathcal{B}^{\text{old}}$ is unchanged. Assume that b_n is not contained in any disc b_j with $j < n$ and, without loss of generality, that b_n intersects $B_1^{\text{old}}, \dots, B_i^{\text{old}}$ but not $B_{i+1}^{\text{old}}, \dots, B_{n-1}^{\text{old}}$, where $0 \leq i \leq n - 1$ (setting $i = 0$ if b_n has no intersection). Then

$B_j^{\text{new}} = B_j^{\text{old}}$ is unchanged for $j = i + 1, \dots, n - 1$, so it suffices below to find the edges of $B_1^{\text{new}}, \dots, B_i^{\text{new}}$ and B_n^{new} .

If $i = 0$ then $B_n^{\text{new}} = b_n$ is an isolated cell with boundary edge ∂b_n . In steps (ii)–(v) we assume that $i \geq 1$.

(ii) *Finding the interior edges of B_n^{new} .* To obtain the interior edges of B_n^{new} , for $j = 1, \dots, i$, we start by assigning $e_{j,n}^{\text{new}} \leftarrow [u_{j,n}^{\text{new}}, v_{j,n}^{\text{new}}]$, considering $u_{j,n}^{\text{new}}$ and $v_{j,n}^{\text{new}}$ as (potential) boundary vertices given by the endpoints of the chord $E_{j,n}$. Furthermore, for $k = 1, \dots, i$ with $k \neq j$, if $e_{j,n}^{\text{new}} \cap H_{n,k} = \emptyset$ (or, equivalently, $u_{j,n}^{\text{new}} \notin H_{n,k}$ and $v_{j,n}^{\text{new}} \notin H_{n,k}$, since $H_{n,k}$ is convex), we obtain $e_{j,n}^{\text{new}} \leftarrow \emptyset$ and we can stop the k -loop, else $e_{j,n}^{\text{new}} \leftarrow e_{j,n}^{\text{new}} \cap H_{n,k}$. In the latter case either both vertices are contained in $H_{n,k}$ and so the edge remains unchanged, or exactly one vertex is not contained in $H_{n,k}$, e.g. $u_{j,n}^{\text{new}} \notin H_{n,k}$ but $v_{j,n}^{\text{new}} \in H_{n,k}$, in which case $u_{j,n}^{\text{new}}$ becomes an interior vertex given by the point $e_{j,n}^{\text{new}} \cap \partial H_{n,k}$ while $v_{j,n}^{\text{new}}$ is unchanged. In this way we find all the interior edges of B_n^{new} , and all the interior and boundary vertices of B_n^{new} .

Since we have assumed that $i > 0$, B_n^{new} is empty if and only if it has no interior edges.

(iii) *Modifying the old interior edges.* At the same time as we do step (ii) above, we also check whether each interior edge $e_{j,k}^{\text{old}} = [u_{j,k}^{\text{old}}, v_{j,k}^{\text{old}}]$ of \mathcal{B}^{old} with $j < k \leq i$ should be kept, reduced, or omitted when we consider \mathcal{B}^{new} (recalling that $e_{j,k}^{\text{new}} = e_{j,k}^{\text{old}}$ is unchanged if $j > i$ or $k > i$). We have

$$e_{j,k}^{\text{new}} = e_{j,k}^{\text{old}} \cap H_{j,n} = e_{j,k}^{\text{old}} \cap H_{k,n}.$$

Thus, $e_{j,k}^{\text{new}}$ is empty if $u_{j,k}^{\text{old}} \notin H_{k,n}$ and $v_{j,k}^{\text{old}} \notin H_{k,n}$, while $e_{j,k}^{\text{new}} = e_{j,k}^{\text{old}}$ if $u_{j,k}^{\text{old}} \in H_{k,n}$ and $v_{j,k}^{\text{old}} \in H_{k,n}$. Furthermore, if $u_{j,k}^{\text{old}} \in H_{k,n}$ and $v_{j,k}^{\text{old}} \notin H_{k,n}$ then $e_{j,k}^{\text{new}} = [u_{j,k}^{\text{old}}, v_{j,k}^{\text{new}}]$, where $v_{j,k}^{\text{new}}$ is the point given by $e_{j,k}^{\text{old}} \cap \partial H_{k,n}$. Similarly, if $u_{j,k}^{\text{old}} \notin H_{k,n}$ and $v_{j,k}^{\text{old}} \in H_{k,n}$ then $e_{j,k}^{\text{new}} = [u_{j,k}^{\text{new}}, v_{j,k}^{\text{old}}]$, where $u_{j,k}^{\text{new}}$ is the point given by $e_{j,k}^{\text{old}} \cap \partial H_{k,n}$.

Note that, for each $j \leq i$, B_j^{new} is empty if and only if it has no interior edge.

(iv) *Finding the boundary edges of B_n^{new} .* Suppose that B_n^{new} has $m > 0$ boundary vertices $w_1^{\text{new}}, \dots, w_m^{\text{new}}$. Note that m is an even number, and we can organize the boundary vertices such that $w_1^{\text{new}} = z_n + r_n(\cos \varphi_1^{\text{new}}, \sin \varphi_1^{\text{new}}), \dots, w_m^{\text{new}} = z_n + r_n(\cos \varphi_m^{\text{new}}, \sin \varphi_m^{\text{new}})$, where $0 \leq \varphi_1^{\text{new}} < \dots < \varphi_m^{\text{new}} < 2\pi$. Then B_n^{new} has $m/2$ boundary edges, namely

$$[w_2^{\text{new}}, w_3^{\text{new}}], [w_4^{\text{new}}, w_5^{\text{new}}], \dots, [w_m^{\text{new}}, w_1^{\text{new}}] \quad \text{if } z_n + (r_n, 0) \in H_{n,j} \text{ for all } j = 1, \dots, i$$

and

$$[w_1^{\text{new}}, w_2^{\text{new}}], [w_3^{\text{new}}, w_4^{\text{new}}], \dots, [w_{m-1}^{\text{new}}, w_m^{\text{new}}] \quad \text{otherwise.}$$

(v) *Modifying the old boundary edges.* Finally, we modify the boundary edges $[u_j^{\text{old}}, v_j^{\text{old}}]$ of \mathcal{B}^{old} considering \mathcal{B}^{new} and $j \leq i$ (noting that $[u_j^{\text{old}}, v_j^{\text{old}}]$ is a boundary edge of \mathcal{B}^{new} too if $j > i$). This is done in a similar way as in step (iv). Suppose that B_j^{new} has $m_j > 0$ boundary vertices $w_1^{\text{new}}, \dots, w_{m_j}^{\text{new}}$, which we organize as in step (iv). Then B_j^{new} has boundary edges

$$[w_2^{\text{new}}, w_3^{\text{new}}], [w_4^{\text{new}}, w_5^{\text{new}}], \dots, [w_{m_j}^{\text{new}}, w_1^{\text{new}}]$$

$$\text{if } z_j + (r_j, 0) \in H_{j,k} \text{ for all } k \leq n \text{ with } k \neq j \text{ and } b_j \cap b_k \neq \emptyset$$

and

$$[w_1^{\text{new}}, w_2^{\text{new}}], [w_3^{\text{new}}, w_4^{\text{new}}], \dots, [w_{m_j-1}^{\text{new}}, w_{m_j}^{\text{new}}] \quad \text{otherwise.}$$

A.2. The case where a disc is deleted

Suppose that we are deleting the disc b_n from a configuration $\{b_1, \dots, b_n\}$ of $n \geq 1$ discs, which are assumed to be in general position. We also assume that we know the power tessellation \mathcal{B}^{old} of $\mathcal{U}^{\text{old}} = \bigcup_1^n b_i$. Below we explain how to construct the new power tessellation \mathcal{B}^{new} of $\mathcal{U}^{\text{new}} = \bigcup_1^{n-1} b_i$. More precisely, with respect to \mathcal{B}^{old} , we assume that we know all the interior edges $[u_{i,j}^{\text{old}}, v_{i,j}^{\text{old}}]$ and all the boundary edges $[u_i^{\text{old}}, v_i^{\text{old}}]$. We want to construct the tessellation \mathcal{B}^{new} of $\mathcal{U}^{\text{new}} = \mathcal{U}^{\text{old}} \setminus b_n$ by finding the interior edges $[u_{i,j}^{\text{new}}, v_{i,j}^{\text{new}}]$ and the boundary edges $[u_i^{\text{new}}, v_i^{\text{new}}]$ associated to each new cell B_i^{new} , noting that B_i^{new} either agrees with B_i^{old} or is an enlargement of B_i^{old} or is a completely new cell. One possibility could be to ‘reverse’ the construction in Section A.1, where a new disc is added; however, we realized that it is easier to create the new edges without reversing the construction in Section A.1 but using a construction as described below. This is partly explained by the fact that an old empty set B_i^{old} may possibly be replaced by a nonempty set B_i^{new} .

(i) *Considering the discs intersecting the disc which is deleted.* Clearly, if B_n^{old} is empty then $\mathcal{B}^{\text{new}} = \mathcal{B}^{\text{old}}$ is unchanged. Assume that B_n^{old} is a nonempty cell and, without loss of generality, that b_n intersects b_1, \dots, b_i but not b_{i+1}, \dots, b_{n-1} , where $0 \leq i \leq n - 1$ (setting $i = 0$ if b_n has no intersection). Then it suffices to find the edges of $B_1^{\text{new}}, \dots, B_i^{\text{new}}$, since $B_j^{\text{new}} = B_j^{\text{old}}$ is unchanged for $j = i + 1, \dots, n - 1$. If $i = 0$ then $B_n^{\text{old}} = b_n$ is an isolated cell, and so $B_1^{\text{new}} = B_1^{\text{old}}, \dots, B_{n-1}^{\text{new}} = B_{n-1}^{\text{old}}$ are unchanged. In the following steps (ii)–(iv), suppose that $i > 0$.

(ii) *Finding the new interior edges.* If $i = 1$, no new interior edge appears. Suppose that $i \geq 2$. We want to determine each set $e_{j,k}^{\text{new}}$ with $j < k \leq i$. We start by assigning all cells $B_1^{\text{new}}, \dots, B_i^{\text{new}}$ to be nonempty and by assigning $e_{j,k}^{\text{new}} \leftarrow [u_{j,k}^{\text{new}}, v_{j,k}^{\text{new}}]$, considering $u_{j,k}^{\text{new}}$ and $v_{j,k}^{\text{new}}$ as (potential) boundary vertices given by the endpoints of the chord $E_{j,k}$. Consider a loop with $l = 1, \dots, i$ and $l \neq j, k$. If $e_{j,k}^{\text{new}} \cap H_{k,l} = \emptyset$ (or, equivalently, $u_{j,k}^{\text{new}} \notin H_{k,l}$ and $v_{j,k}^{\text{new}} \notin H_{k,l}$, since $H_{k,l}$ is convex), we find that $e_{j,k}^{\text{new}}$ is empty and we can stop the l -loop. Otherwise, assign $e_{j,k}^{\text{new}} \leftarrow e_{j,k}^{\text{new}} \cap H_{k,l}$, where we note that only the following two cases can occur. First, if both vertices of $e_{j,k}^{\text{new}}$ are contained in $H_{k,l}$, the edge remains unchanged. Second, if exactly one vertex is not contained in $H_{k,l}$, e.g. $u_{j,k}^{\text{new}} \notin H_{k,l}$ but $v_{j,k}^{\text{new}} \in H_{k,l}$, then $u_{j,k}^{\text{new}}$ becomes an interior vertex given by the point $e_{j,k}^{\text{new}} \cap \partial H_{k,l}$ while $v_{j,k}^{\text{new}}$ is unchanged. When the loop is finished, we have determined all the new interior edges, including the information whether their endpoints are interior or boundary vertices.

(iii) *Determining the new cells.* For each $j \leq i$, we determine if B_j^{new} is a new cell by checking if it has an edge. Suppose that B_j^{new} has no interior edge, i.e. it is either an empty set or a new isolated cell. If an arbitrary fixed point of b_j is included in $H_{j,l}$ for all $l = 1, \dots, n - 1$ with $l \neq j$ then B_j has exactly one boundary edge and it is an isolated cell. Otherwise, B_j^{new} is empty. In this way we determine whether each B_j^{new} is empty or a new cell, including whether it is an isolated cell.

(iv) *Finding the new boundary edges.* We have already determined the new isolated boundary edges in step (iii). Consider a nonisolated cell B_j^{new} with $j \leq i$ with boundary vertices $w_k^{\text{new}} = z_j + r_j(\cos \varphi_k^{\text{new}}, \sin \varphi_k^{\text{new}})$, $k = 1, \dots, m_j$. Recall that $m_j > 0$ is an even number and we organize the vertices so that $0 \leq \varphi_1^{\text{new}} < \dots < \varphi_{m_j}^{\text{new}} < 2\pi$; cf. step (iv) in Section A.1. Then B_j^{new} has $m_j/2$ boundary edges, namely

$$[w_2^{\text{new}}, w_3^{\text{new}}], [w_4^{\text{new}}, w_5^{\text{new}}], \dots, [w_{m_j}^{\text{new}}, w_1^{\text{new}}] \quad \text{if } z_j + (r_j, 0) \in H_{j,l} \text{ for all } l = 1, \dots, i$$

and

$$[w_1^{\text{new}}, w_2^{\text{new}}], [w_3^{\text{new}}, w_4^{\text{new}}], \dots, [w_{m_j-1}^{\text{new}}, w_{m_j}^{\text{new}}] \quad \text{otherwise.}$$

Acknowledgements

We are grateful to Lars Døvling Andersen, Herbert Edelsbrunner, and Wilfrid Kendall for useful comments. Supported by the Danish Natural Science Research Council, grant 272-06-0442, ‘Point process modelling and statistical inference’, and by grants GAČR 201/06/0302 and GAČR 201/05/H007.

References

- [1] AURENHAMMER, F. (1987). Power diagrams: properties, algorithms and applications. *SIAM J. Comput.* **16**, 78–96.
- [2] BADDELEY, A. AND MØLLER, J. (1989). Nearest-neighbour Markov point processes and random sets. *Internat. Statist. Rev.* **2**, 89–121.
- [3] BADDELEY, A. J. AND VAN LIESHOUT, M. N. M. (1995). Area-interaction point processes. *Ann. Inst. Statist. Math.* **46**, 601–619.
- [4] BADDELEY, A. J., VAN LIESHOUT, M. N. M. AND MØLLER, J. (1996). Markov properties of cluster processes. *Adv. Appl. Prob.* **28**, 346–355.
- [5] BARNDORFF-NIELSEN, O. E. (1978). *Information and Exponential Families in Statistical Theory*. John Wiley, Chichester.
- [6] CHAN, K. S. AND GEYER, C. J. (1994). Discussion of the paper ‘Markov chains for exploring posterior distributions’ by Luke Tierney. *Ann. Statist.* **22**, 1747.
- [7] CHIN, Y. C. AND BADDELEY, A. J. (2000). Markov interacting component processes. *Adv. Appl. Prob.* **32**, 597–619.
- [8] CRESSIE, N. A. C. (1993). *Statistics for Spatial Data*, 2nd edn. John Wiley, New York.
- [9] DIGGLE, P. (1981). Binary mosaics and the spatial pattern of heather. *Biometrics* **37**, 531–539.
- [10] EDELSBRUNNER, H. (1995). The union of balls and its dual shape. *Discrete Computational Geometry* **13**, 415–440.
- [11] EDELSBRUNNER, H. (2004). Biological applications of computational topology. In *Handbook of Discrete and Computational Geometry*, eds J. Goodman and J. O’Rourke, Chapman & Hall/CRC, Boca Raton, FL, pp. 1395–1412.
- [12] GEORGI, H.-O. (1976). Canonical and grand canonical Gibbs states for continuum systems. *Commun. Math. Phys.* **48**, 31–51.
- [13] GEYER, C. J. (1999). Likelihood inference for spatial point processes. In *Stochastic Geometry: Likelihood and Computation*, eds O. E. Barndorff-Nielsen *et al.*, Chapman & Hall/CRC, Boca Raton, FL, pp. 79–140.
- [14] GEYER, C. J. AND MØLLER, J. (1994). Simulation procedures and likelihood inference for spatial point processes. *Scand. J. Statist.* **21**, 359–373.
- [15] HÄGGSTRÖM, O., VAN LIESHOUT, M. N. M. AND MØLLER, J. (1999). Characterization results and Markov chain Monte Carlo algorithms including exact simulation for some spatial point processes. *Bernoulli* **5**, 641–659.
- [16] HALL, P. (1988). *Introduction to the Theory of Coverage Processes*. John Wiley, New York.
- [17] HANISCH, K.-H. (1981). On classes of random sets and point processes. *Serdica* **7**, 160–167.
- [18] KENDALL, W. S. (1990). A spatial Markov property for nearest-neighbour Markov point processes. *J. Appl. Prob.* **28**, 767–778.
- [19] KENDALL, W. S. (1998). Perfect simulation for the area-interaction point process. In *Probability Towards 2000* (Springer Lecture Notes Statist. **128**), eds L. Accardi and C. Heyde, Springer, New York, pp. 218–234.
- [20] KENDALL, W. S. (2004). Geometric ergodicity and perfect simulation. *Electron. Commun. Prob.* **9**, 140–151.
- [21] KENDALL, W. S. AND MØLLER, J. (2000). Perfect simulation using dominating processes on ordered spaces, with application to locally stable point processes. *Adv. Appl. Prob.* **32**, 844–865.
- [22] KENDALL, W. S., VAN LIESHOUT, M. AND BADDELEY, A. (1999). Quermass-interaction processes: conditions for stability. *Adv. Appl. Prob.* **31**, 315–342.
- [23] KLEIN, W. (1982). Potts-model formulation of continuum percolation. *Phys. Rev. B* **26**, 2677–2678.
- [24] LIKOS, C., MECKE, K. AND WAGNER, H. (1995). Statistical morphological of random interfaces in microemulsions. *J. Chem. Phys.* **102**, 9350–9361.
- [25] MECKE, K. (1994). *Integralgeometrie in der Statistischen Physik* (Reine Physik **25**). Harri Deutsch, Frankfurt.
- [26] MECKE, K. (1996). A morphological model for complex fluids. *J. Phys. Condensed Matters* **8**, 9663–9667.

- [27] MOLCHANOV, I. (1997). *Statistics of the Boolean Model for Practitioners and Mathematicians*. John Wiley, Chichester.
- [28] MØLLER, J. (1994). Contribution to the discussion of N. L. Hjort and H. Omre (1994): Topics in spatial statistics. *Scand. J. Statist.* **21**, 346–349.
- [29] MØLLER, J. (1994). *Lectures on Random Voronoi Tessellations* (Lecture Notes Statist. **87**). Springer, New York.
- [30] MØLLER, J. (1999). Markov chain Monte Carlo and spatial point processes. In *Stochastic Geometry: Likelihood and Computation* (Monogr. Statist. Appl. Prob. **80**), ed. O. E. Barndorff-Nielsen, Chapman & Hall/CRC, Boca Raton, FL, pp. 141–172.
- [31] MØLLER, J. AND HELISOVÁ, K. (2007). Power diagrams and interaction processes for unions of discs. Res. Rept. R-2007-15, Department of Mathematical Sciences, Aalborg University.
- [32] MØLLER, J. AND HELISOVÁ, K. (2008). Likelihood inference for unions of interacting discs. In preparation.
- [33] MØLLER, J. AND WAAGEPETERSEN, R. P. (1998). Markov connected component fields. *Adv. Appl. Prob.* **30**, 1–35.
- [34] MØLLER, J. AND WAAGEPETERSEN, R. P. (2003). *Statistical Inference and Simulation for Spatial Point Processes*. Chapman & Hall/CRC, Boca Raton, FL.
- [35] NGUYEN, X. X. AND ZESSIN, H. (1979). Integral and differential characterizations of Gibbs processes. *Math. Nachr.* **88**, 105–115.
- [36] OKABE, A., BOOTS, B., SUGIHARA, K. AND CHIU, S. N. (2000). *Spatial Tessellations. Concepts and Applications of Voronoi Diagrams*. 2nd edn. John Wiley, Chichester.
- [37] PRESTON, C. J. (1977). Spatial birth-and-death processes. *Bull. Internat. Statist. Inst.* **46**, 371–391.
- [38] RIPLEY, B. D. AND KELLY, F. P. (1977). Markov point processes. *J. London Math. Soc.* **15**, 188–192.
- [39] ROBERTS, G. O. AND ROSENTHAL, J. S. (1997). Geometric ergodicity and hybrid Markov chains. *Electron. Commun. Probab.* **2**, 13–25.
- [40] RUELLE, D. (1971). Existence of a phase transition in a continuous classical system. *Phys. Rev. Lett.* **27**, 1040–1041.
- [41] STOYAN, D., KENDALL, W. S. AND MECKE, J. (1995). *Stochastic Geometry and Its Applications*, 2nd edn. John Wiley, Chichester.
- [42] VAN LIESHOUT, M. N. M. (2000). *Markov Point Processes and Their Applications*. Imperial College Press, London.
- [43] WEIL, W. AND WIEACKER, J. (1984). Densities for stationary random sets and point processes. *Adv. Appl. Prob.* **16**, 324–346.
- [44] WEIL, W. AND WIEACKER, J. (1988). A representation theorem for random sets. *Prob. Math. Statist.* **9**, 147–151.
- [45] WIDOM, B. AND ROWLINSON, J. S. (1970). a new model for the study of liquid-vapor phase transitions. *J. Chem. Phys.* **52**, 1670–1684.
- [46] WILSON, R. (1972). *Introduction to Graph Theory*. Oliver and Boyd, Edinburgh.